Spatial landmarks regulate a Cdc42-dependent MAPK pathway to control differentiation and the response to positional compromise

Sukanya Basu[a,1], Nadia Vadaie[a,1], Aditi Prabhakar[a], Boyang Li[a], Hema Adhikari[a], Andrew Pitoniak[a], Jacky Chow[a], Colin A. Chavel[a], and Paul J. Cullen[a,2]

[a]Department of Biological Sciences, University at Buffalo, Buffalo, NY 14260

Edited by Jasper Rine, University of California, Berkeley, CA, and approved February 22, 2016 (received for review November 17, 2015)

A fundamental problem in cell biology is to understand how spatial information is recognized and integrated into morphogenetic responses. Budding yeast undergoes differentiation to filamentous growth, which involves changes in cell polarity through mechanisms that remain obscure. Here we define a regulatory input where spatial landmarks (bud-site–selection proteins) regulate the MAPK pathway that controls filamentous growth (fMAPK pathway). The bud-site GTPase Rsr1p regulated the fMAPK pathway through Cdc24p, the guanine nucleotide exchange factor for the polarity establishment GTPase Cdc42p. Positional landmarks that direct Rsr1p to bud sites conditionally regulated the fMAPK pathway, corresponding to their roles in regulating bud-site selection. Therefore, cell differentiation is achieved in part by the reorganization of polarity at bud sites. In line with this conclusion, dynamic changes in budding pattern during filamentous growth induced corresponding changes in fMAPK activity. Intrinsic compromise of bud-site selection also impacted fMAPK activity. Therefore, a surveillance mechanism monitors spatial position in response to extrinsic and intrinsic stress and modulates the response through a differentiation MAPK pathway.

spatial cues | GTPase | polarity establishment | polar landmarks | MAPK

Positional information is critical for the establishment of polarity and the regulation of cell division. Spatial context is also important for many biological processes, including development, neuronal organization and guidance, directional motility, and cell differentiation. Positional information comes from proteins that mark the cell-surface and gradients of diffusible receptors, peptide ligands, and transcription factors (1–4). Evolutionarily conserved protein modules control cell polarity in eukaryotes (5, 6). In yeast, polarity is determined by cell type. Positional cues mark the poles of haploid and diploid cells, which are recognized by a core module composed of the bud-site GTPase Rsr1p (7), its guanine nucleotide exchange factor Bud5p (8, 9), and its GTPase activating protein Bud2p (10). Rsr1p in turn regulates the ubiquitous polarity establishment GTPase Cdc42p (11). Active (GTP-bound) Cdc42p associates with multiple effector proteins to initiate and maintain polarized growth at specific sites.

Cell polarity can be reorganized in response to extrinsic cues. Yeast cells can orient their axis of growth along pheromone gradients (12) and to the site of a wound (13). Cell polarity is also reorganized during filamentous/invasive/pseudohyphal growth, which occurs in response to nutrient limitation (glucose or nitrogen), and which results in the formation of branched chains of interconnected cells (14–16). Many fungal species undergo filamentous growth, and in some species of pathogenic microorganisms, filamentous growth is required for virulence (17). In yeast, the change in polarity during filamentous growth is striking in haploid cells, which switch from axial to distal-unipolar budding (15, 18). It is not clear how polarity is reorganized during filamentous growth, except that signal transduction pathways are involved and the same positional cues that regulate bud-site selection in diploid cells are also required for filamentous growth (19, 20).

Among the signaling pathways that regulate filamentous growth is an ERK-type MAPK pathway called the filamentous growth (fMAPK) pathway. MAPK pathways are evolutionarily conserved protein modules that regulate cell differentiation and stress responses in eukaryotes. The fMAPK pathway is regulated by the signaling mucin Msb2p (21), a cell-surface glycoprotein that is proteolytically processed and activated in glucose-limiting conditions (22, 23). At the plasma membrane (PM), Msb2p functions with transmembrane proteins Sho1p (21, 24, 25) and Opy2p (26–33). The transmembrane regulators connect (in some manner) to a cytosolic scaffold-type adaptor, Bem4p, that also regulates the fMAPK pathway (34–36). Msb2p and Bem4p associate with Cdc42p (21, 34) to promote its function in the fMAPK pathway (37, 38). Like many Rho GTPases (39–42), Cdc42p has multiple roles in regulating cell polarity and signaling. In the fMAPK pathway, Cdc42p regulates a protein kinase cascade composed of Ste20p (PAK), Ste11p (MAPKKK), Ste7p (MAPKK), and Kss1p (MAPK) (43, 44). Kss1p regulates a suite of transcription factors (45–47) that control the expression of target genes, whose products together with other proteins and pathways generate the filamentous cell type.

Here we report a new regulatory connection between bud-site–selection proteins and the fMAPK pathway. We show that the bud-site GTPase Rsr1p, together with positional landmarks, regulate the fMAPK pathway through the shared GTPase Cdc42p. This is a new role for bud-site–selection proteins in regulating MAPK signaling. Following-up on this discovery led to the identification of a surveillance mechanism, where positional cues provide information about spatial context to regulate the cellular response to extrinsic and intrinsic morphogenetic stress. In this way, cells monitor positional integrity before engaging in MAPK-dependent differentiation and other responses.

Significance

We identify a new role for bud-site–selection proteins outside of their established roles in regulating growth site determination, as components of a surveillance pathway that monitors spatial position during intrinsic and extrinsic morphogenetic stress and regulates a Cdc42p- and MAPK-dependent response.

Author contributions: S.B., N.V., A. Prabhakar, and P.J.C. designed research; S.B., N.V., A. Prabhakar, B.L., H.A., A. Pitoniak, and P.J.C. performed research; B.L. and J.C. contributed new reagents/analytic tools; S.B., N.V., A. Prabhakar, C.A.C., and P.J.C. analyzed data; and P.J.C. wrote the paper.

The authors declare no conflict of interest.

This article is a PNAS Direct Submission.

[1]S.B. and N.V. contributed equally to this work.

[2]To whom correspondence should be addressed. Email: pjcullen@buffalo.edu.

This article contains supporting information online at www.pnas.org/lookup/suppl/doi:10.1073/pnas.1522679113/-/DCSupplemental.

Results

Bud-Site GTPase Rsr1p Regulates the fMAPK Pathway. Rsr1p is an established regulator of bud-site selection that functions through Cdc42p (7, 10, 48). Rsr1p was also uncovered in a screen for Cdc42p-interacting proteins that impact fMAPK activity (34). To determine whether Rsr1p regulates the fMAPK pathway, the *rsr1*Δ mutant was examined in a strain background that undergoes filamentous/invasive growth (∑1278b) (14, 49), a fungal behavioral response that is controlled by the fMAPK pathway. In this background, the *rsr1*Δ mutant was defective for phosphorylation of the MAP kinase Kss1p (P~Kss1p) (Fig. 1*A*) and showed the same defect as a null mutant in the fMAPK pathway (*ste11*Δ). The *ste11*Δ, *ste12*Δ and *ste20*Δ mutants have equivalent phenotypes in filamentous growth assays and were used interchangeably. The *rsr1*Δ mutant was defective for invasive growth (Fig. 1*B*) by the plate-washing assay (15). The *rsr1*Δ mutant was also defective for expression of transcriptional targets of the fMAPK pathway, including *FRE-lacZ* (Fig. 1*C* and *SI Appendix*, Fig. S1*A*) (44), *FLO11* (see below), and *FUS1-HIS3* (*SI Appendix*, Fig. S1*B*), which in ∑1278b cells lacking an intact mating pathway (*ste4*) shows dependency on fMAPK regulators (21, 34).

The fMAPK pathway also regulates the response to defects in protein glycosylation (28, 50, 51). To determine whether Rsr1p is involved in this aspect of fMAPK regulation, a conditional glycosylation mutant, *pmi40-101*, whose glycosylation defect is suppressed by mannose (50), was examined. Rsr1p was required for fMAPK activity in the *pmi40-101* mutant experiencing glycosylation deficiency (Fig. 1*D* and *SI Appendix*, Fig. S1*C*). In this blot and other blots, total Kss1p levels can vary as a result of positive feedback, because *KSS1* is a transcriptional target of the fMAPK pathway (52). Together, the results show that Rsr1p positively regulates the fMAPK pathway.

Rsr1p Controls the fMAPK Pathway by Nucleotide Cycling and Interaction with the Guanine Nucleotide Exchange Factor Cdc24p. Rsr1p regulates bud-site selection through the Cdc42p module (7). To determine whether Rsr1p regulates the fMAPK pathway through Cdc42p, the amount of active Cdc42p (Cdc42p-GTP) in the cell was increased by disrupting *RGA1*, which encodes the main GTPase activating protein for Cdc42p in the fMAPK pathway (53, 54). The *rga1*Δ *rsr1*Δ double-mutant bypassed the fMAPK signaling defect of the *rsr1*Δ single-mutant (Fig. 2*A*), which indicates that Rsr1p functions at or above the level of Cdc42p in the fMAPK pathway. The *rga1*Δ mutant did not rescue the bud-site–selection defect of the *rsr1*Δ mutant (*SI Appendix*, Table S3). Thus, bypass occurs by raising Cdc42p-GTP levels, not restoring the bud-site–selection defect of *rsr1*Δ.

Rsr1p is a Ras-type GTPase that cycles between active (GTP-bound) and inactive (GDP-bound) conformations. In the GTP-bound conformation, Rsr1p interacts with effector proteins. A version of Rsr1p that fails to interact with effectors (T35A) (55–57) or versions that mimic the GDP- (K16N) or GTP-locked states (G12V) were defective for fMAPK activity (Fig. 2*B*). A GTP-locked version of Rsr1p might be expected to constitutively activate the fMAPK pathway. However, cells containing $Rsr1p^{G12V}$ have a bud-site–selection defect (*SI Appendix*, Table S3) that results from sequestering Cdc24p in the inactive state (7) and from its failure to concentrate at polarized sites (56). Thus, as for many GTPases, nucleotide cycling of Rsr1p is necessary for its function in the fMAPK pathway. The G12V, K16N, and T35A versions of Rsr1p have a dominant-negative phenotype, which induces a bud-site–selection defect in wild-type cells (55). The G12V, K16N, and T35A versions of Rsr1p also caused a defect in fMAPK activity in wild-type cells (Fig. 2*C*).

During bud-site selection, Rsr1p recruits Cdc24p to the PM (56, 58, 59). A version of Cdc24p that is constitutively anchored to the PM by myristoylation (Myr-Cdc24p) (34) bypassed the fMAPK signaling defect of the *rsr1*Δ mutant (Fig. 2*D*). Myr-Cdc24p also bypassed the signaling defect of the *bud4*Δ mutant (*SI Appendix*, Fig. S1*D*). Together, these results indicate that one function for bud-site–selection proteins in fMAPK regulation is PM recruitment of Cdc24p. Rsr1p also interacts with Cdc24p at bud sites (7, 58, 60, 61). To determine whether Rsr1p regulates the fMAPK pathway through interaction with Cdc24p, a version of Cdc24p was examined that at permissive temperatures cannot interact with Rsr1p (*cdc24-4* or G168D) (58). Cells harboring the *cdc24-4* allele showed reduced fMAPK pathway activity (Fig. 2*D*) [p*cdc24-4* (30 °C)]. Thus, Rsr1p interacts with and recruits Cdc24p to the PM to regulate the fMAPK pathway.

All of the versions of Rsr1p tested that were defective for bud-site selection were defective for fMAPK activity, which may indicate that bud-site selection itself is tied to fMAPK regulation. To test this possibility, a version of Rsr1p was examined that lacked the polybasic domain, which mediates homotypic interactions (56, 57, 62),

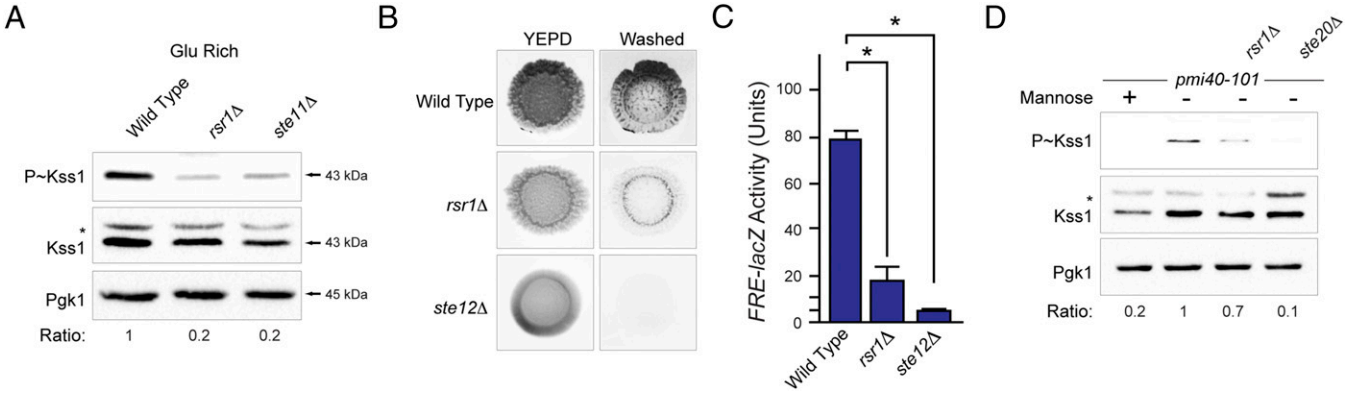

Fig. 1. Rsr1p regulates the fMAPK pathway. (*A*) Immunoblot analysis of P~Kss1p levels in wild-type cells and the *rsr1*Δ and *ste11*Δ mutants. Cells were grown to midlog phase in SD+AA (glucose-rich media). Cell extracts were examined by immnoblot analysis using p42/p44 antibodies (to detect P~Kss1p), Kss1p antibodies, and Pgk1p antibodies as a control for protein levels. Numbers indicate relative band intensity for P~Kss1p to total Kss1p (Ratio). Asterisk refers to a background band (102). (*B*) Plate-washing assay. Cells were grown for 96 h on YEPD medium. The plate was photographed, washed, and photographed again. (*C*) Expression of the *FRE-lacZ* reporter. Cells were grown to midlog phase in SD-URA medium to maintain selection for the plasmid and evaluated by β-galactosidase assays. β-Galactosidase assays were performed from independent cultures and are expressed in Miller Units. Error bars show differences between samples. *$P < 0.05$. (*D*) Strains harboring the *pmi40-101* mutation alone and with the indicated deletions were grown to midlog phase in YEPD or YEPD + 50 mM mannose. P~Kss1p levels were examined as in *A*.

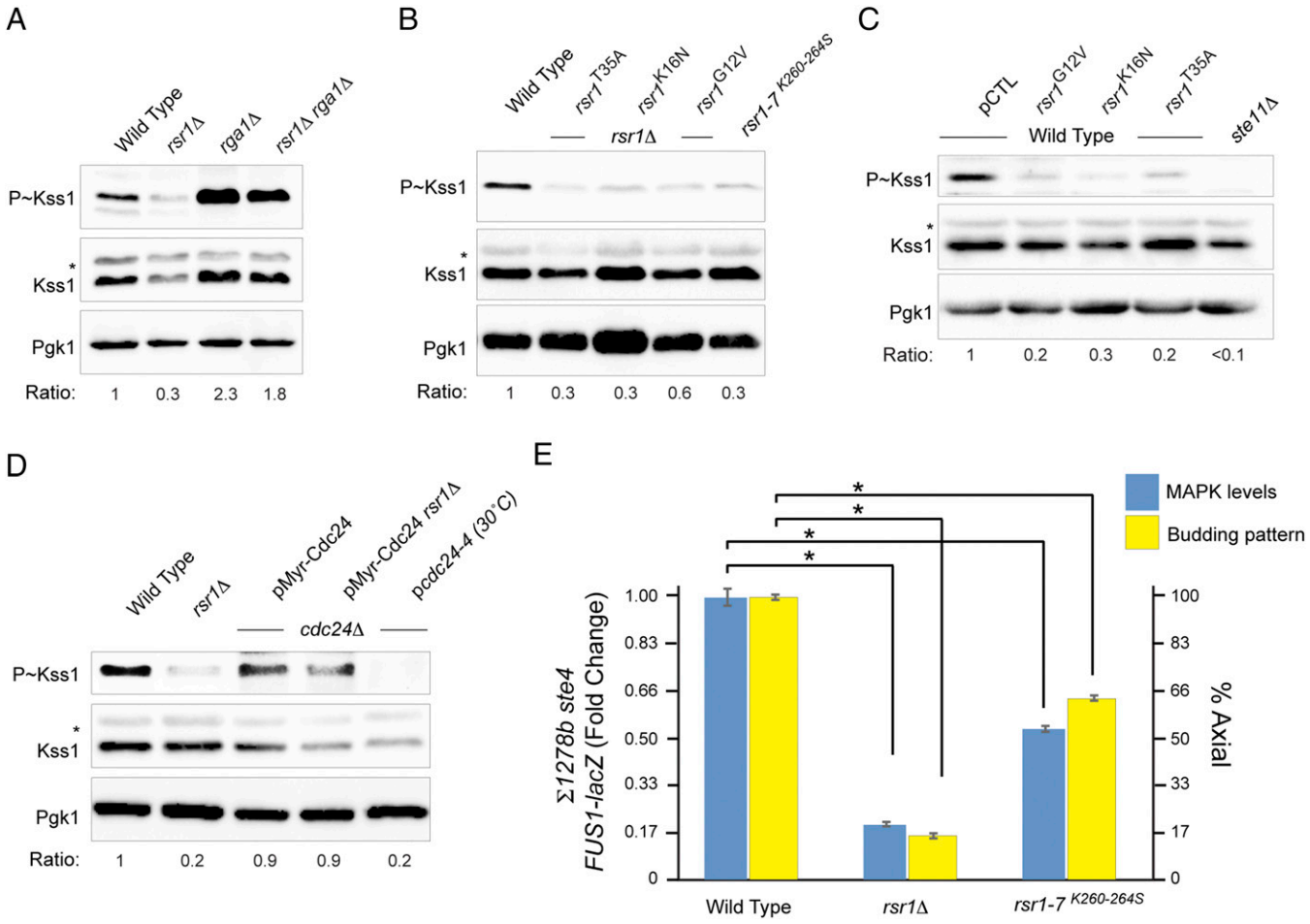

Fig. 2. Rsr1p regulates the fMAPK pathway through GTPase cycling and interaction with Cdc24p. (*A*) P~Kss1p levels were examined as in Fig. 1*A* for the strains indicated. Cells were grown to midlog phase in SD+AA. (*B*) P~Kss1p levels were examined as in Fig. 1*A*, except that cells were grown in SD-URA or SD-LEU media to maintain selection for plasmids harboring alleles of *RSR1*. (*C*) P~Kss1p levels were examined as in Fig. 1*A* in wild-type cells harboring the indicated *RSR1* alleles. Cells were grown to midlog phase in YEPD media. (*D*) P~Kss1p levels were examined as in Fig. 1*A* in the *cdc24::NAT* and *cdc24::NAT rsr1*Δ strains carrying YEp351-*Cdc24p-GFP* (wild-type), pRS425-*CDC24-4* (*cdc24-4*), and YEp351-*MYR-Cdc24p-GFP* (Myr-Cdc24p) plasmids. (*E*, *Left* axis) β-Galactosidase assays were performed as described in Fig. 1*C*. Wild-type values were set to 1. Other values were adjusted accordingly. The experiment was performed in triplicate. Error bars show the SD between trials. (*Right* axis) Axial budding expressed as a percentage was determined for wild-type cells, *rsr1*Δ, and *rsr1-7*$^{K260\text{-}264S}$ mutants grown to midlog phase in SD-URA medium. Budding pattern was determined by CFW staining. More than 200 cells were counted in independent trials. Error bars show the SD between trials. **P* < 0.01.

and that was defective for fMAPK activity (Fig. 2*B*) (*rsr1-7*$^{K260\text{-}264S}$). The *rsr1-7* mutant has a conditional bud-site–selection defect (62). In our hands, the defect was less severe than reported (62), which might result from differences in growth conditions or strain backgrounds. The partial bud-site–selection defect of the *rsr1-7*$^{K260\text{-}264S}$ mutant (Fig. 2*E*, yellow bars) showed a corresponding defect in fMAPK activity (Fig. 2*E*, blue bars). These results, and results presented below show a correspondence between bud-site selection and fMAPK activity.

Axial Cues Regulate the fMAPK Pathway in Glucose-Rich Conditions. During bud-site selection, Rsr1p is recruited by positional landmarks to bud sites (11). We asked whether positional landmarks also regulate the fMAPK pathway. In glucose-rich conditions (2% glucose), haploids bud in an axial pattern (Fig. 3*A*) (63). A mutant lacking axial cues showed a defect in fMAPK activity in glucose-rich conditions (Fig. 3*B*, *axl2*Δ, blue bars), based on the expression of the fMAPK pathway target *FLO11* (64). The *axl2*Δ mutant showed the same defect as the core module (Fig. 3*B*, *rsr1*Δ, blue bars) and the same genetic suppression pattern as the *rsr1*Δ *rga1*Δ double-mutant (Fig. 3*C*; compare with Fig. 2*A* and *SI Appendix*, Table S3). Like *axl2*Δ, other axial mutants were also defective for fMAPK activity, based on P~Kss1p analysis and *FUS1* reporter activity (*SI Appendix*, Fig. S2).

Two additional experiments support the idea that axial cues regulate the fMAPK pathway. First, restoring axial budding to axial mutants by loss of multigenerational cortical marks (Rax proteins) (65–67) restored MAPK signaling (*SI Appendix*, Fig. S3 *A–D*, and Table S4). The Rax proteins might impact fMAPK through multiple mechanisms, as these proteins localize to the division site as well as the distal pole (65–67). Rax proteins have not been extensively studied in haploid cells. Consistent with their roles in regulating distal-pole budding in diploid cells, Rax1p and Rax2p regulated invasive growth (*SI Appendix*, Fig. S3*E*) and distal-pole budding of filamentous haploid cells (*SI Appendix*, Fig. S3*F*).

A second experiment supporting a role for axial cues in regulating fMAPK comes from analysis of separate functional domains on the Axl2p protein. In addition to its role in regulating bud-site selection, Axl2p also interacts with Cdc42p and plays a role in regulating septin organization. This role for Axl2p was uncovered by its ability to suppress the septin organization defects of an allele

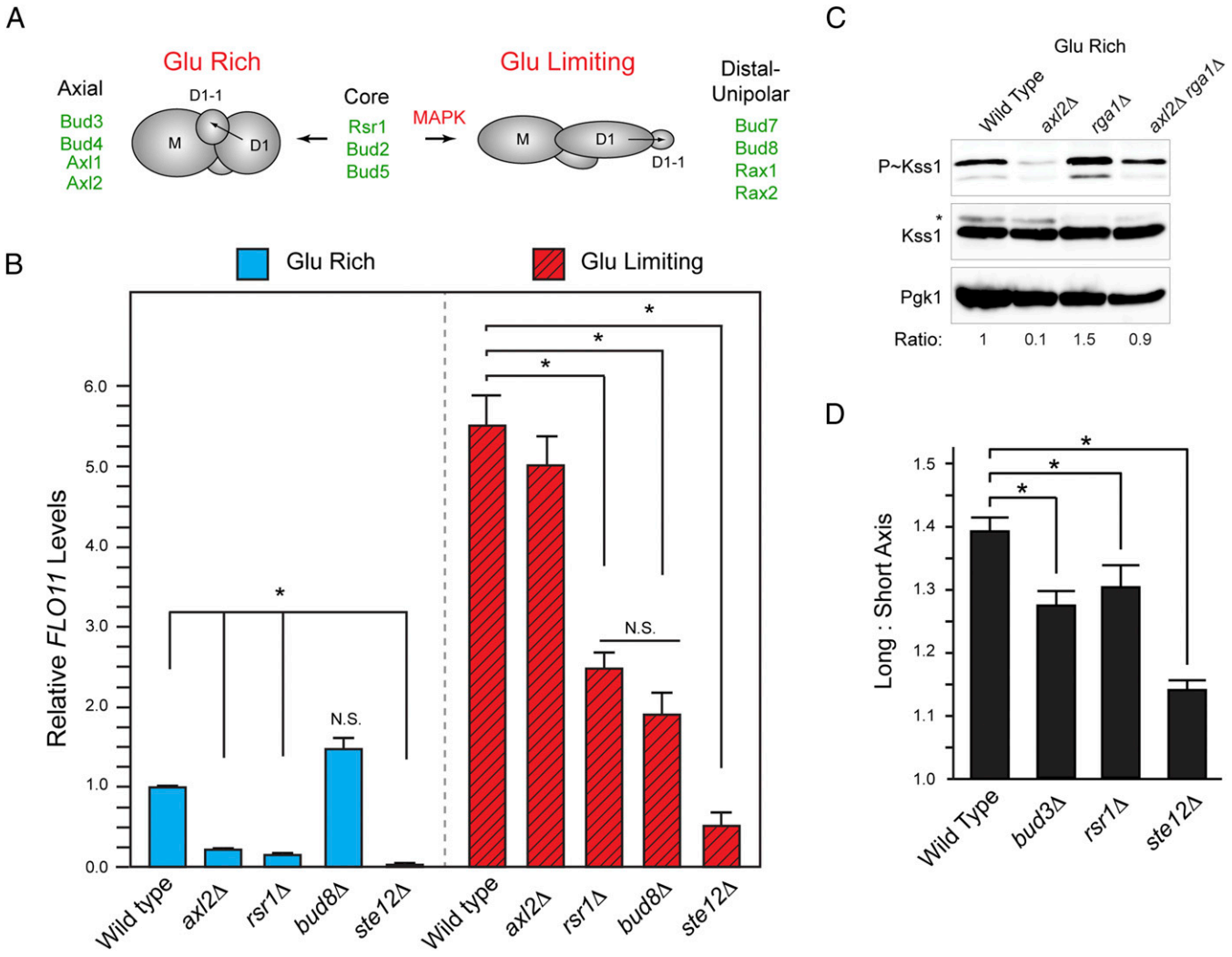

Fig. 3. Bud-site–selection proteins conditionally regulate the fMAPK pathway depending on glucose availability. (*A*) Budding pattern of haploid cells in glucose-rich and glucose-limiting conditions (Glu, glucose). Proteins required for axial budding, distal-unipolar budding, and the core module are shown. (*B*) Quantitative PCR (qPCR) analysis of *FLO11* expression (relative to *ACT1* levels) in the indicated mutants in glucose-rich (YEPD) and glucose-limiting (YEP-Gal) conditions. Assays were performed from independent cultures. Average values are shown. Error bars show the SD between trials. *$P < 0.01$. (*C*) P~Kss1p levels were examined as in Fig. 1*A* for the indicated strains. Cells were grown to midlog phase in YEPD medium. NS, not significant. (*D*) Ratio of the long-to-short axis in the indicated mutants. More than 50 cells were counted for each mutant. Cells were incubated in glucose-limiting media (YEP + 0.2% glucose). *$P < 0.001$.

of *CDC42* called *cdc42*^{V36G} (68). A version of Axl2p that is specifically defective for septin organization functioned in the fMAPK pathway (*SI Appendix*, Fig. S4 *A* and *B*) (p1-544, 641–725) (68, 69). By comparison, a version of Axl2p that is specifically defective for axial budding did not (*SI Appendix*, Fig. S4 *A* and *B*) (p1-544, 641–685). This version of Axl2p (p1-544, 641–685) lacks an interaction site for Bud4p but retains the ability to localize to the mother-bud neck (68). Therefore, the bud-site–selection function of Axl2p underlies its role in regulating the fMAPK pathway. These results reinforce the idea that axial cues regulate the fMAPK pathway.

Why do axial cues regulate fMAPK in an environment where cells do not normally undergo filamentous growth (Fig. 3*A*, Glu Rich)? Basal activity of the fMAPK pathway in glucose-rich conditions prepares cells for invasive growth (70). Specifically, at high and moderate glucose levels, cells express *FLO11*, which promotes adhesion during biofilm/mat formation (71) and contributes to the initiation of filamentous growth. As glucose levels decrease, cells become elongated through a mechanism that involves the polarisome (20) and a delay in the cell cycle (72, 73), although cells continue to bud axially (70). Axial cues (*bud3*Δ) and the core module (*rsr1*Δ) were required for cell elongation (Fig. 3*D*), which occurs in an fMAPK-dependent manner during filamentous growth (Fig. 3*D*) (*ste12*Δ) (72, 74). Axial cues were also required for the fMAPK response to protein glycosylation deficiency (*SI Appendix*, Fig. S4*C*). Therefore, axial cues regulate basal fMAPK activity in glucose-rich conditions to prepare cells for invasive growth and contribute to the diversity of MAPK-dependent responses, like the response to protein glycosylation deficiency.

Bud8p Regulates the fMAPK Pathway In Glucose-Limiting Conditions. Glucose depletion triggers invasive growth (18) and activates the fMAPK pathway (Fig. 3*B*, compare blue bar to red bar for wild-type) (31). In glucose-limiting conditions, haploid cells switch from axial to distal-unipolar budding by utilization of the distal-pole marker Bud8p (Fig. 3*A*) (20). Bud8p was required for *FLO11* expression in glucose-limiting conditions (Fig. 3*B*, compare wild-type to *bud8*Δ, red bars). Bud8p was also required for P~Kss1p activity (*SI Appendix*, Fig. S4*D*). Therefore, Bud8p regulates the fMAPK pathway in glucose-limiting conditions.

In glucose-rich conditions, Bud8p is not required for budding in haploid cells (63). Under this condition, Bud8p did not regulate the fMAPK pathway (Fig. 3*B*, *bud8*Δ, blue bars, and *SI Appendix*, Fig. S2). Similarly, axial cues, which do not regulate distal-pole budding under nutrient-limiting conditions (63), did not regulate *FLO11* expression in glucose-limiting conditions (Fig. 3*B*, *axl2*Δ, red bars). The core module is required for bud-site selection under all conditions (63) and regulated fMAPK signaling under all conditions tested (Fig. 3*B*, *rsr1*Δ, blue and red bars). Therefore, different positional landmarks regulate the fMAPK pathway in different nutrient states corresponding to their roles in regulating bud-site selection.

A Specific Input from the Rsr1p Branch Regulates the fMAPK Pathway. Msb2p and other proteins regulate Cdc42p in the fMAPK pathway (see Fig. 7, discussed below) (21, 22, 34). To define how inputs from the Msb2p and Rsr1p branches impact the fMAPK pathway, the *msb2*Δ and *rsr1*Δ single-mutants were compared with an *msb2*Δ *rsr1*Δ double-mutant and MAPK-null mutant (*ste11*Δ). In glucose-rich conditions, Msb2p and Rsr1p both regulated the fMAPK pathway (Fig. 4*A* and *SI Appendix*, Fig. S5*A*). In glucose-limiting conditions, *rsr1*Δ played a more minor role (Fig. 4*B*). This observation supports the data presented in Fig. 3*B*, which shows that axial and core mutants have a fivefold decrease in MAPK activity in glucose-rich conditions [Fig. 3*B*, blue bars, compare wild-type to *rsr1*Δ and *axl2*Δ (although the pathway is activated to a lower overall level)], compared with a ∼1.8-fold decrease seen in distal and core mutants under glucose-limiting conditions (Fig. 3*B*, red bars, compare wild-type to *rsr1*Δ and *bud8*Δ). Thus, bud-site–selection proteins play quantitatively different roles in regulating the fMAPK pathway under different conditions.

Msb2p is activated in glucose-limiting conditions by proteolytic processing (23), which may partially obviate the requirement for the Rsr1p branch. In support of this possibility, a hyperactive allele of *MSB2*, *MSB2*$^{\Delta 100-818}$ (21), bypassed the fMAPK signaling defect of the *rsr1*Δ mutant (Fig. 4*C* and *SI Appendix*, Fig. S5*B*). Similarly, a hyperactive version of Sho1p, Sho1p^{P120L} (22) also bypassed the fMAPK signaling defect of the *rsr1*Δ mutant (*SI Appendix*, Fig. S5*C*). Hyperactive versions of Msb2p and Sho1p also bypassed the signaling (*SI Appendix*, Fig. S5*D*) and invasive growth (*SI Appendix*, Fig. S5*E*) defects of the *axl2*Δ mutant. Therefore, the Rsr1p branch can be bypassed by activation of the Msb2p branch.

Like other signaling pathways, the fMAPK pathway shares components with other MAPK pathways, including the mating and high osmolarity glycerol response (HOG) pathways (75–78). Despite using common components, each MAPK pathway induces a specific response (52). In the mating pathway, Rsr1p does not regulate MAPK signaling but contributes to cell polarization [e.g., the formation of cells with mating projections or shmoos (79)]. Rsr1p and Gβγ-Far1p-Cdc24p have a redundant function in cell polarization during mating (79–81), and Rsr1p becomes essential for shmoo formation in cells with defective Gβγ-mediated chemotropism (80). We also found that Rsr1p did not regulate the mating pathway, based on sensitivity of cells to the mating pheromone α factor (Fig. 4*D*) and P∼MAPK analysis (*SI Appendix*, Fig. S6*A*). To determine whether Rsr1p regulates the HOG pathway, the *RSR1* gene was disrupted in cells lacking the redundant Sln1p branch (*ssk1*Δ) (82). The *rsr1*Δ *ssk1*Δ double-mutant showed

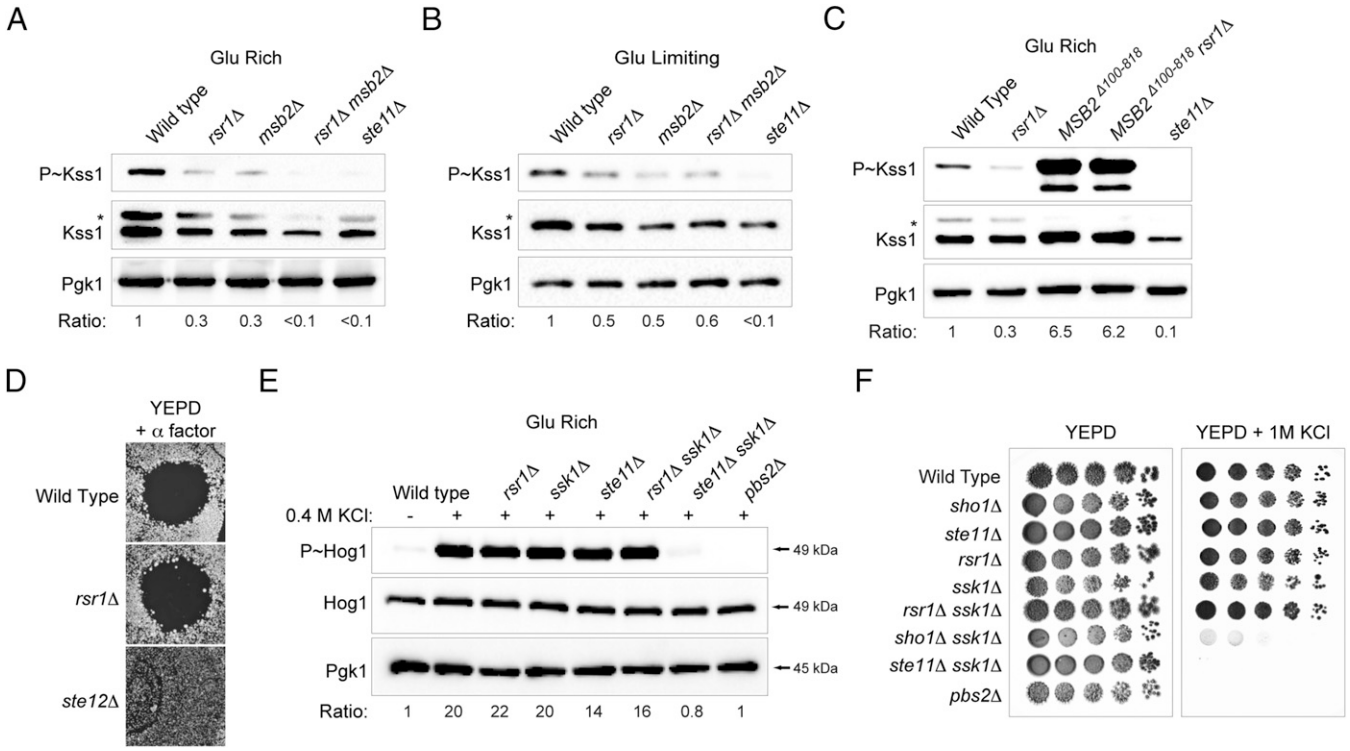

Fig. 4. Roles of the Rsr1p and Msb2p branches in regulating the fMAPK pathway and other MAPK pathways that share components. (*A*) P∼Kss1p levels were examined as in Fig. 1*A* for the strains indicated. Cells were grown in SD+AA medium to midlog phase. (*B*) P∼Kss1p levels were examined as in Fig. 1*A* for the strains indicated. Cells were induced in YEP-GAL medium to midlog phase. (*C*) P∼Kss1p analysis of Msb2$^{\Delta 100-818}$ signaling in wild-type cells and the *rsr1*Δ mutant. P∼Kss1p levels were examined as in Fig. 1*A*. Cells were grown in SD+AA medium to midlog phase. (*D*) Halo assays. Approximately equal concentrations of the indicated strains were spread onto YEPD media. Next, 5 μm of α-factor was spotted onto plates, which were incubated for 48 h at 30 °C. The experiment was performed four times and a typical example is shown. (*E*) P∼Hog1p levels in the indicated mutants. Cells were grown to midlog phase in YEPD. KCl was added to a final concentration of 0.4 M for 10 min. Cell extracts were evaluated by immunoblot analysis using antibodies that recognize P∼p38, Hog1p, and Pgk1p proteins. Ratio refers to P∼Hog1p to Hog1p levels. (*F*) Serial dilutions were spotted onto YEPD and YEPD + 1 M KCl for 3 d at 30 °C.

normal phosphorylation of the MAPK Hog1p in response to salt (P~Hog1p) (Fig. 4*E*, compare *rsr1*Δ *ssk1*Δ to *ste11*Δ *ssk1*Δ and *pbs2*Δ, which lacks the HOG MAPKK). Moreover, the *rsr1*Δ *ssk1*Δ mutant did not show a growth defect in high-salt medium (Fig. 4*F*). Thus, Rsr1p does not regulate the HOG pathway. In fact, basal cross-talk to the fMAPK pathway that occurs in the *pbs2*Δ mutant (24, 83), which requires fMAPK components, was also dependent on Rsr1p (*SI Appendix*, Fig. S6*B*). We also tested whether general defects in cell polarity might influence fMAPK activity. Mutants defective for polarized growth [e.g., polarisome mutants *bud6*Δ, *pea2*Δ, *spa2*Δ and *bni1*Δ (84)] or that exhibit hyperpolarized growth [*hsl1*Δ and *hsl7*Δ (85)] did not impact fMAPK (*SI Appendix*, Fig. S6*C*). Therefore, bud-site–selection proteins play a specific role in regulating the fMAPK pathway.

Yeast Cells Dynamically Orient Their Growth Site Based on Glucose Levels, Which Has a Corresponding Impact on fMAPK Activity. The fact that bud-site–selection proteins regulate the fMAPK pathway indicates that spatial/positional information itself may control aspects of the differentiation response. Except for the observation that prolonged nutrient starvation leads to loss of axial budding in haploids (63), the dynamics of nutrient-dependent changes in polarity in haploid cells has not been explored. To define the rate of polarity reorganization during filamentous growth, a two-fluorescent staining technique was used (86). Midlog phase cells shifted from glucose-rich (YEPD) to glucose-limiting [YEP-Galactose (Gal)] conditions switched from axial (>99%) to distal-unipolar budding (~50%) after 2.5 h (Fig. 5*A*, red square, and *SI Appendix*, Fig. S7). Cells shifted from YEP-Gal back to YEPD reverted to axial budding in a similar timespan (Fig. 5*A*, green triangle). Cells shifted from YEPD to YEPD in a mock experiment remained axial (Fig. 5*A*, yellow circle). Examples of the two-fluorescent staining technique are shown in Fig. 5*B*. Given that doubling time is ~2.5 h, these results indicate that yeast cells survey glucose availability and orient their axis of growth within a growth cycle.

Time-lapse microscopy showed that cells transferred from YEPD to YEP-GAL switched from axial to distal-unipolar budding in a single cycle (Movies S1 and S2). Most haploid cells bud distally in glucose-limited media, as evident by the single-cell invasive growth assay (Fig. 5*C*, *Upper*) (18). Filamentous cells

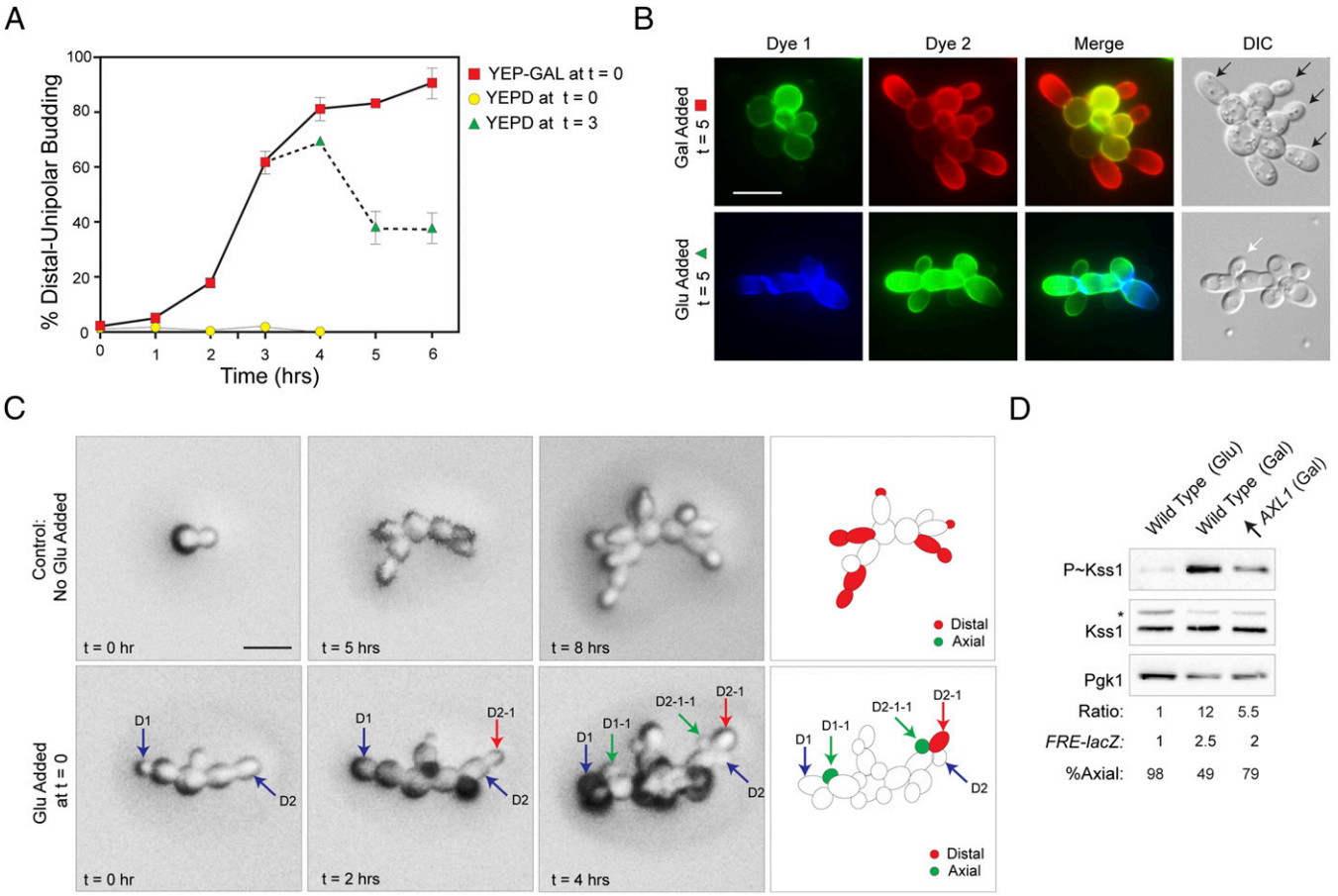

Fig. 5. Extrinsic changes in spatial position regulate changes in fMAPK activity. (*A*) Distal-unipolar budding (%) was determined in cells grown in different conditions. At time 0, midlog phase cells in YEPD were harvested, washed, and transferred to YEPD (yellow circle) or YEP-Gal (red square) medium. At the indicated times, cell aliquots were evaluated for distal-unipolar buds by two-fluorescent staining. For the switchback experiment, cells grown in YEP-Gal for 3 h were transferred to YEPD medium and evaluated for distal-pole budding (green triangle). At least 50 cells were counted for each experiment. Error bars show SD between separate trials. (*B*) Examples of FITC-ConA/TRITC-ConA double-labeling (*Upper*) and CFW/FITC-ConA double-labeling (*Lower*) of cells from the 5-h time point. Distal buds are marked with black arrows. The axial bud in the lower panel is marked with a white arrow. (Scale bar, 5 μm.) (*C*, *Upper*) Example of the budding pattern of filamentous cells by the single cell assay. (Scale bar, 10 μm). (*Lower*) Time course of budding pattern of filamentous cells exposed to glucose. Cell D1 budded at the proximal pole, D1-1. Cell D2 budded at the distal pole (D2-1). D2-1 budded at the proximal pole D2-1-1. Diagram at right illustrates the budding pattern. Red, distal-unipolar; green, axial. Pattern was confirmed by serial images taken in the plane of the *z* axis. (*D*) P~Kss1p levels were examined as in Fig. 1*A* for the strains indicated. Wild-type cells were grown in YEPD (Glu) or YEP-Gal (Gal). ↑*AXL1* refers to p*Gal-AXL1*. Cells were also evaluated for *FRE-lacZ* activity. β-Galactosidase assays were performed as described in Fig. 1*C*. Differences in *FRE-lacZ* activity are expressed as a ratio (wild-type set to 1), and differences between trials were <10%. More than 200 cells were counted for each strain to determine percent axial.

exposed to glucose switched to axial budding (Fig. 5*C*, *Lower*, D1 produced D1-1, and *SI Appendix*, Fig. S8). Not all cells switched (Fig. 5*C*, *Lower*, D2 produced D2-1, and *SI Appendix*, Fig. S8), but produced daughters that budded axially in the following cycle (Fig. 5*C*, D2-1 produced D2-1-1). Large cells typically retained the distal pattern, which may indicate that commitment to bud distally occurs at a specific point in the cell cycle. The switch in polarity is not a result of changes in the marks themselves, which are present under all conditions (*SI Appendix*, Fig. S9), but may be controlled by Axl1p, a cell-type specific protein that is required for axial budding (87, 88) whose levels are regulated by glucose availability (20).

Because budding pattern impacts fMAPK activity (Figs. 1–4), the switch in polarity in response to glucose availability may have a corresponding impact on MAPK signaling. In support of this possibility, cells forced to bud axially in glucose-limiting conditions (by overexpressing *AXL1*) (Fig. 5*D*, % Axial) showed reduced P~Kss1p levels (Fig. 5*D*) and *FRE-lacZ* activity (Fig. 5*D*, *FRE-lacZ*). These results suggest the possibility that the switch to axial budding by filamentous cells encountering a glucose-rich environment provides a mechanism for attenuation of the fMAPK pathway. Cell polarity reorganization can therefore dictate MAPK activity in response to an extrinsic cue.

Intrinsic Compromise of Bud-Site Selection Impacts fMAPK Activity. The above data indicate that bud-site–selection proteins may monitor the spatial position of the cell and regulate a MAPK-dependent response. In addition to extrinsic cues like glucose, budding pattern is tied to intrinsic processes such as transcription, cell cycle progression, cytoskeletal organization, phosphatidylinositol phosphate signaling, cytokinesis, and protein trafficking (89, 90). The above findings predict that mutants in these processes that confer bud-site–selection defects would show reduced fMAPK activity. This prediction is based on the correspondence between budding pattern and fMAPK activity in cells compromised for Rsr1p, Bud2p, Bud3p, Bud4p, Bud5p, Bud7p, Bud8p, Axl1p, Axl2p, and Rax function (Figs. 1–4 and *SI Appendix*, Figs. S2 and S3). To further test this possibility, a mutant was examined in which bud-site selection was compromised, in a process not otherwise connected to fMAPK regulation. At permissive temperatures, the septin mutant (*cdc12-6*) displays normal cytokinesis but has a bud-site–selection defect (Fig. 6*A*, % Axial), which may result from mis-localization of axial cues at the mother-bud neck (91). The bud-site–selection defect of the *cdc12*-6 mutant corresponded to a defect in fMAPK activity (Fig. 6*A*). Defects in phosphatidylinositol phosphate signaling, which also compromises bud-site selection, likewise compromised fMAPK signaling, which can account for a previous result from our laboratory (92). Therefore, intrinsic compromise of bud-site selection attenuates fMAPK activity.

What if the regulatory input by bud-site–selection proteins is ignored? To test this possibility, bypass of the signaling defect of bud-site–selection mutants was examined. Cells expressing $MSB2^{\Delta 100–818}$, which signals independent of the Rsr1p branch (Fig. 4*C* and *SI Appendix*, Fig. S5*B*), had irregular morphologies, including growth at multiple sites (Fig. 6*B*). This phenotype does not occur in wild-type cells because of singularity in budding (93, 94) but has been reported in cells expressing activated versions of Cdc42p (94, 95). Such cells showed localization of GFP-Bud8p at multiple sites (Fig. 6*C*) and had multiple septin rings (Fig. 6*C*), indicative of multiple mother-bud necks. Cells with elevated fMAPK activity, like $MSB2^{\Delta 100–818}$ or cells that overexpress the *MSB2* gene (*GAL-MSB2*), which also bypasses *rsr1*Δ, showed growth defects over multiple passages (Fig. 6*D*), which indicates that this growth pattern is not optimal for viability. Therefore, bypassing the regulatory input of the Rsr1p branch leads to growth and polarity defects.

Discussion

Bud-site–selection proteins are among the most intensively studied positional landmarks in eukaryotes, and the molecular basis for how they function is well understood (11). Bud-site–selection proteins

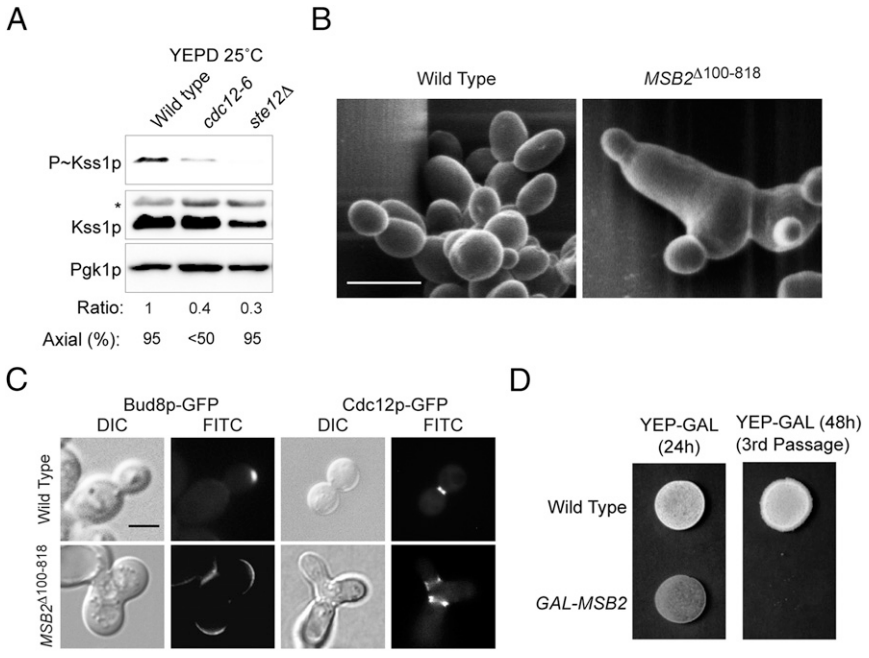

Fig. 6. Intrinsic compromise of spatial position impacts fMAPK activity. (*A*) P~Kss1p levels were examined as in Fig. 1*A* for the strains indicated. Budding pattern was determined by bud-scar staining and visual inspection. More than 200 cells were counted for the experiment. (*B*) Scanning electron micrographs of wild-type cells (*Left*) and cells with an activated fMAPK pathway (*Right*). (Scale bar, 5 μm.) (*C*) Localization of GFP-Bud8p and Cdc12p-GFP (103) in cells expressing $MSB2^{\Delta 100–818}$. (Scale bar, 5 μm.) (*D*) Growth defect of the indicated yeast strains spotted onto YEP-GAL for the times shown overexpressing *MSB2* over multiple passages.

are not known to function outside the budding pathway. Here we define a new role for bud-site–selection proteins as regulators of an ERK-type MAPK pathway. To our knowledge, this is the first connection between positional landmarks and MAPK regulation in yeast and may extend broadly to other systems. This connection does not arise from a moonlighting function of a particular bud-site–selection protein but involves the entire bud-site–selection machinery. We further identify a surveillance mechanism that allows cells to sense spatial information and control a Cdc42p- and MAPK-dependent response.

Spatial Cues Regulate the fMAPK Pathway. The discovery that bud-site–selection proteins regulate the fMAPK pathway builds on the understanding of how the fMAPK is regulated. Two regulatory branches converge on the Cdc42p module to regulate the fMAPK pathway: the Msb2p branch, which also contains Sho1p, Opy2p and Bem4p (21, 24, 26–34), and the Rsr1p branch, whose activity is governed by positional landmarks (Fig. 7).

A potentially trivial explanation is that bud-site–selection proteins elevate the level of Cdc42p-GTP in the fMAPK pathway. Indeed, Rsr1p interacts with Cdc24p and functions at the level of Cdc42p. Two observations, however, indicate that Rsr1p plays a specific role in fMAPK regulation. One is that Rsr1p exhibits a nonadditive input to the fMAPK pathway (Fig. 4*A*). Thus, the Rsr1p and Msb2p branches cooperate to transmit a signal to fMAPK. The second observation is that Rsr1p regulates the fMAPK pathway but not other MAPK pathways that share components (Fig. 4 *D–F* and *SI Appendix*, Fig. S6*A*). Bud-site–selection proteins may selectively regulate Cdc42p in the fMAPK pathway through Bem4p. Bem4p and Rsr1p interact, based on a two-hybrid screen for cell polarity regulators (Fig. 7, dashed line between Rsr1p and Bem4p) (96), and both proteins bind to Cdc24p. Rsr1p interacts with the CH domain of Cdc24p, which has an auto-inhibitory function (58), and Bem4p binds to the autoregulatory PH-like domain of Cdc24p (34). Thus, Bem4p and Rsr1p may cooperatively regulate Cdc42p by binding separate autoregulatory domains in Cdc24p. Alternatively, Rsr1p may initiate Cdc24p activation at bud sites early in the cell cycle that is sustained by Bem4p. The salient finding from this study is that spatial information is integrated into the fMAPK pathway through a shared GTPase module.

Bud-Site–Selection Proteins as Coincidence Detectors of Nutrient Status. We also show that positional landmarks conditionally regulate the fMAPK pathway in a manner that corresponds to their nutrient-dependent functions in bud-site selection. Glucose levels feed into the fMAPK pathway in two ways (Fig. 7). One is by changes in the glycosylation of Msb2p that occur under nutrient-limiting conditions, resulting in elevated processing of under-glycosylated Msb2p and fMAPK pathway activation (23). This mechanism involves the unfolded protein response. The other is by differential recognition of positional landmarks in different nutrient states. Axial position is an indicator of nutrient surplus, whereas distal-pole budding is an indicator of starvation.

At the distal pole, signaling and position-dependent budding are coordinated. Sho1p interacts with Bud8p (Fig. 7, dashed line between Bud8p and Sho1p) (22), and the proteins localize to the distal pole (70, 97). The fMAPK pathway and other pathways regulate Bud8p-dependent bud-site selection (20). The interaction between signaling and polarity proteins at the distal pole may cluster signaling machinery at the site where polarity reorganization occurs. It is plausible that other bud-site–selection proteins make specific contacts with fMAPK regulators to modulate the signaling response. Such interactions may contribute to a pathway-specific response.

Regulation of Spatial Integrity by a Surveillance Pathway. We show that a surveillance mechanism monitors spatial position and executes a MAPK-dependent response to extrinsic and intrinsic cues. As discussed above, extrinsic changes in glucose levels lead to quantitatively

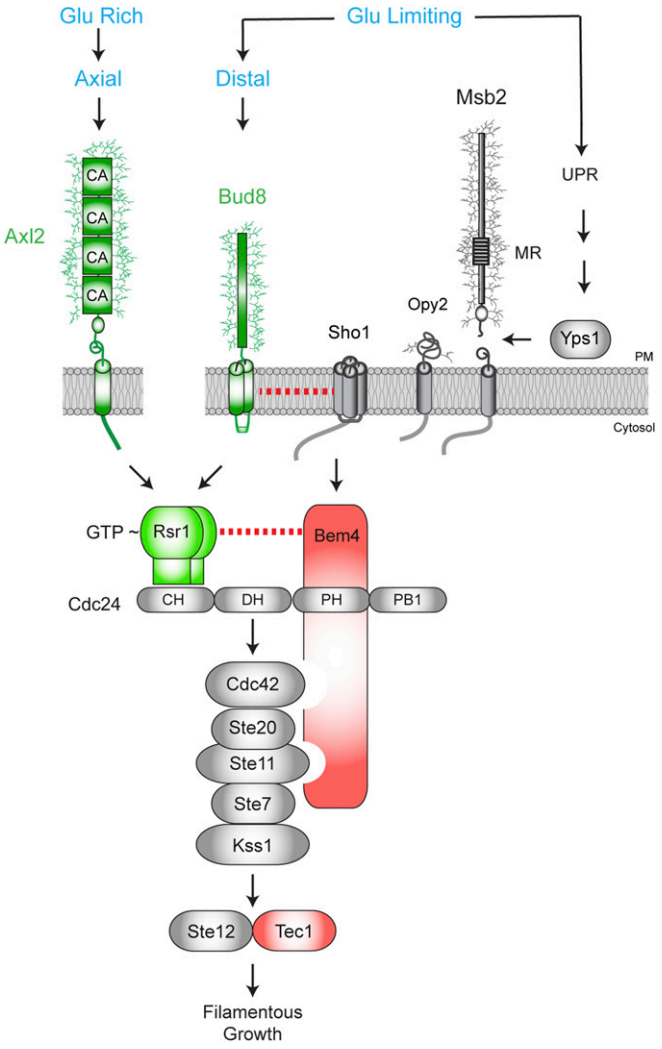

Fig. 7. Model of the fMAPK pathway with inputs from bud-site–selection proteins. In glucose-rich conditions, axial cues (Bud3p, Bud4p, Axl1p, and Axl2p; Axl2p is shown) regulate Cdc24p in the filamentous growth pathway through Rsr1p. Msb2p, Sho1p, Opy2p, and Bem4p also regulate the fMAPK pathway through Cdc42p. In glucose-limiting conditions, Bud8p regulates Rsr1p-dependent activation of the filamentous growth pathway. Glucose limitation also induces processing of Msb2p by Yps1p, which leads to Cdc24p activation through Sho1p and Bem4p. Msb2p, Bud8p, and Axl2p are glycosylated proteins; CA, cadherin-like repeats; MR, mucin repeats; UPR, unfolded protein response.

different signaling from axial and distal cues. We also show that intrinsic problems with bud-site selection, such as in mutants where bud-site selection is compromised, lead to attenuation of the fMAPK pathway. In this way, cells compromised for spatial integrity dampen MAPK signaling until the cell gets its bearings. The regulatory mechanism defined here may extend to other systems. Positional marks have been identified in filamentous fungal species (98) and have been shown to influence cell polarity and virulence in human (99, 100) and plant fungal pathogens (101). It may be interesting to define how such cues impact regulatory pathways to control pathogenic differentiation programs. Spatial cues may generally impact signaling pathways to remodel cell fate and mount responses to compromised positional integrity.

ACKNOWLEDGMENTS. We thank Drs. John Pringle (Stanford University), Charlie Boone (University of Toronto), Erfei Bi (University of Pennsylvania), Hay-Oak Park (Ohio State University), Rong Li (Kansas City Medical Center), Hiten Madhani (University of California, San Francisco), Kenneth Wolfe (Trinity University), Peter Pryciak (University of Massachusetts), Stan Fields (University of Washington), and

Danny Lew (Duke University) for reagents and comments; and Laura Grell, Alexander Bowitch, Lauren Hartley, and Heather Dionne for helping with experiments. The work was supported by National Institutes of Health Grant GM098629.

1. Molofsky AV, et al. (2014) Astrocyte-encoded positional cues maintain sensorimotor circuit integrity. *Nature* 509(7499):189–194.
2. Paré AC, et al. (2014) A positional Toll receptor code directs convergent extension in *Drosophila*. *Nature* 515(7528):523–527.
3. Tautz D (1988) Regulation of the *Drosophila* segmentation gene hunchback by two maternal morphogenetic centres. *Nature* 332(6161):281–284.
4. Gregor T, Tank DW, Wieschaus EF, Bialek W (2007) Probing the limits to positional information. *Cell* 130(1):153–164.
5. Li R, Bowerman B (2010) Symmetry breaking in biology. *Cold Spring Harb Perspect Biol* 2(3):a003475.
6. Kohwi M, Doe CQ (2013) Temporal fate specification and neural progenitor competence during development. *Nat Rev Neurosci* 14(12):823–838.
7. Park HO, Bi E, Pringle JR, Herskowitz I (1997) Two active states of the Ras-related Bud1/Rsr1 protein bind to different effectors to determine yeast cell polarity. *Proc Natl Acad Sci USA* 94(9):4463–4468.
8. Chant J, Corrado K, Pringle JR, Herskowitz I (1991) Yeast BUD5, encoding a putative GDP-GTP exchange factor, is necessary for bud site selection and interacts with bud formation gene *BEM1*. *Cell* 65(7):1213–1224.
9. Bender A (1993) Genetic evidence for the roles of the bud-site-selection genes BUD5 and BUD2 in control of the Rsr1p (Bud1p) GTPase in yeast. *Proc Natl Acad Sci USA* 90(21):9926–9929.
10. Park HO, Chant J, Herskowitz I (1993) BUD2 encodes a GTPase-activating protein for Bud1/Rsr1 necessary for proper bud-site selection in yeast. *Nature* 365(6443): 269–274.
11. Bi E, Park HO (2012) Cell polarization and cytokinesis in budding yeast. *Genetics* 191(2):347–387.
12. Segall JE (1993) Polarization of yeast cells in spatial gradients of alpha mating factor. *Proc Natl Acad Sci USA* 90(18):8332–8336.
13. Kono K, Saeki Y, Yoshida S, Tanaka K, Pellman D (2012) Proteasomal degradation resolves competition between cell polarization and cellular wound healing. *Cell* 150(1):151–164.
14. Gimeno CJ, Ljungdahl PO, Styles CA, Fink GR (1992) Unipolar cell divisions in the yeast *S. cerevisiae* lead to filamentous growth: Regulation by starvation and RAS. *Cell* 68(6):1077–1090.
15. Roberts RL, Fink GR (1994) Elements of a single MAP kinase cascade in *Saccharomyces cerevisiae* mediate two developmental programs in the same cell type: Mating and invasive growth. *Genes Dev* 8(24):2974–2985.
16. Pan X, Harashima T, Heitman J (2000) Signal transduction cascades regulating pseudohyphal differentiation of *Saccharomyces cerevisiae*. *Curr Opin Microbiol* 3(6): 567–572.
17. Polvi EJ, Li X, O'Meara TR, Leach MD, Cowen LE (2015) Opportunistic yeast pathogens: Reservoirs, virulence mechanisms, and therapeutic strategies. *Cell Mol Life Sci* 72(12):2261–2287.
18. Cullen PJ, Sprague GF, Jr (2000) Glucose depletion causes haploid invasive growth in yeast. *Proc Natl Acad Sci USA* 97(25):13619–13624.
19. Taheri N, Köhler T, Braus GH, Mösch HU (2000) Asymmetrically localized Bud8p and Bud9p proteins control yeast cell polarity and development. *EMBO J* 19(24): 6686–6696.
20. Cullen PJ, Sprague GF, Jr (2002) The roles of bud-site-selection proteins during haploid invasive growth in yeast. *Mol Biol Cell* 13(9):2990–3004.
21. Cullen PJ, et al. (2004) A signaling mucin at the head of the Cdc42- and MAPK-dependent filamentous growth pathway in yeast. *Genes Dev* 18(14):1695–1708.
22. Vadaie N, et al. (2008) Cleavage of the signaling mucin Msb2 by the aspartyl protease Yps1 is required for MAPK activation in yeast. *J Cell Biol* 181(7):1073–1081.
23. Adhikari H, et al. (2015) Role of the unfolded protein response in regulating the mucin-dependent filamentous growth MAPK pathway. *Mol Cell Biol* 35(8): 1414–1432.
24. O'Rourke SM, Herskowitz I (1998) The Hog1 MAPK prevents cross talk between the HOG and pheromone response MAPK pathways in *Saccharomyces cerevisiae*. *Genes Dev* 12(18):2874–2886.
25. Tatebayashi K, et al. (2015) Osmosensing and scaffolding functions of the oligomeric four-transmembrane domain osmosensor Sho1. *Nat Commun* 6:6975.
26. Wu C, Jansen G, Zhang J, Thomas DY, Whiteway M (2006) Adaptor protein Ste50p links the Ste11p MEKK to the HOG pathway through plasma membrane association. *Genes Dev* 20(6):734–746.
27. Ekiel I, et al. (2009) Binding the atypical RA domain of Ste50p to the unfolded Opy2p cytoplasmic tail is essential for the high-osmolarity glycerol pathway. *Mol Biol Cell* 20(24):5117–5126.
28. Yang HY, Tatebayashi K, Yamamoto K, Saito H (2009) Glycosylation defects activate filamentous growth Kss1 MAPK and inhibit osmoregulatory Hog1 MAPK. *EMBO J* 28(10):1380–1391.
29. Yamamoto K, Tatebayashi K, Tanaka K, Saito H (2010) Dynamic control of yeast MAP kinase network by induced association and dissociation between the Ste50 scaffold and the Opy2 membrane anchor. *Mol Cell* 40(1):87–98.
30. Cappell SD, Dohlman HG (2011) Selective regulation of MAP kinase signaling by an endomembrane phosphatidylinositol 4-kinase. *J Biol Chem* 286(17):14852–14860.
31. Karunanithi S, Cullen PJ (2012) The filamentous growth MAPK pathway responds to glucose starvation through the Mig1/2 transcriptional repressors in *Saccharomyces cerevisiae*. *Genetics* 192(3):869–887.
32. Herrero de Dios C, Román E, Diez C, Alonso-Monge R, Pla J (2013) The transmembrane protein Opy2 mediates activation of the Cek1 MAP kinase in *Candida albicans*. *Fungal Genet Biol* 50:21–32.
33. Adhikari H, Caccamise LM, Pande T, Cullen PJ (2015) Comparative analysis of transmembrane regulators of the filamentous growth MAPK pathway uncovers functional and regulatory differences. *Eukaryot Cell* 14(9):868–883.
34. Pitoniak A, et al. (2015) Cdc42p-interacting protein Bem4p regulates the filamentous-growth mitogen-activated protein kinase pathway. *Mol Cell Biol* 35(2):417–436.
35. Hirano H, et al. (1996) ROM7/BEM4 encodes a novel protein that interacts with the Rho1p small GTP-binding protein in *Saccharomyces cerevisiae*. *Mol Cell Biol* 16(8): 4396–4403.
36. Mack D, et al. (1996) Identification of the bud emergence gene BEM4 and its interactions with rho-type GTPases in *Saccharomyces cerevisiae*. *Mol Cell Biol* 16(8): 4387–4395.
37. Leberer E, et al. (1997) Functional characterization of the Cdc42p binding domain of yeast Ste20p protein kinase. *EMBO J* 16(1):83–97.
38. Peter M, Neiman AM, Park HO, van Lohuizen M, Herskowitz I (1996) Functional analysis of the interaction between the small GTP binding protein Cdc42 and the Ste20 protein kinase in yeast. *EMBO J* 15(24):7046–7059.
39. Hanna S, El-Sibai M (2013) Signaling networks of Rho GTPases in cell motility. *Cell Signal* 25(10):1955–1961.
40. McCormack J, Welsh NJ, Braga VM (2013) Cycling around cell-cell adhesion with Rho GTPase regulators. *J Cell Sci* 126(Pt 2):379–391.
41. Ratheesh A, Priya R, Yap AS (2013) Coordinating Rho and Rac: The regulation of Rho GTPase signaling and cadherin junctions. *Prog Mol Biol Transl Sci* 116:49–68.
42. Wilson KF, Erickson JW, Antonyak MA, Cerione RA (2013) Rho GTPases and their roles in cancer metabolism. *Trends Mol Med* 19(2):74–82.
43. Cook JG, Bardwell L, Thorner J (1997) Inhibitory and activating functions for MAPK Kss1 in the *S. cerevisiae* filamentous-growth signalling pathway. *Nature* 390(6655): 85–88.
44. Madhani HD, Styles CA, Fink GR (1997) MAP kinases with distinct inhibitory functions impart signaling specificity during yeast differentiation. *Cell* 91(5):673–684.
45. Cook JG, Bardwell L, Kron SJ, Thorner J (1996) Two novel targets of the MAP kinase Kss1 are negative regulators of invasive growth in the yeast *Saccharomyces cerevisiae*. *Genes Dev* 10(22):2831–2848.
46. Madhani HD, Fink GR (1997) Combinatorial control required for the specificity of yeast MAPK signaling. *Science* 275(5304):1314–1317.
47. van der Felden J, Weisser S, Brückner S, Lenz P, Mösch HU (2014) The transcription factors Tec1 and Ste12 interact with coregulators Msa1 and Msa2 to activate adhesion and multicellular development. *Mol Cell Biol* 34(12):2283–2293.
48. Bender A, Pringle JR (1989) Multicopy suppression of the cdc24 budding defect in yeast by CDC42 and three newly identified genes including the ras-related gene RSR1. *Proc Natl Acad Sci USA* 86(24):9976–9980.
49. Liu H, Styles CA, Fink GR (1996) *Saccharomyces cerevisiae* S288C has a mutation in FLO8, a gene required for filamentous growth. *Genetics* 144(3):967–978.
50. Cullen PJ, et al. (2000) Defects in protein glycosylation cause SHO1-dependent activation of a STE12 signaling pathway in yeast. *Genetics* 155(3):1005–1018.
51. Lee BN, Elion EA (1999) The MAPKKK Ste11 regulates vegetative growth through a kinase cascade of shared signaling components. *Proc Natl Acad Sci USA* 96(22): 12679–12684.
52. Roberts CJ, et al. (2000) Signaling and circuitry of multiple MAPK pathways revealed by a matrix of global gene expression profiles. *Science* 287(5454):873–880.
53. Smith GR, Givan SA, Cullen P, Sprague GF, Jr (2002) GTPase-activating proteins for Cdc42. *Eukaryot Cell* 1(3):469–480.
54. Stevenson BJ, Rhodes N, Errede B, Sprague GF, Jr (1992) Constitutive mutants of the protein kinase STE11 activate the yeast pheromone response pathway in the absence of the G protein. *Genes Dev* 6(7):1293–1304.
55. Ruggieri R, et al. (1992) RSR1, a ras-like gene homologous to Krev-1 (smg21A/rap1A): Role in the development of cell polarity and interactions with the Ras pathway in *Saccharomyces cerevisiae*. *Mol Cell Biol* 12(2):758–766.
56. Park HO, Kang PJ, Rachfal AW (2002) Localization of the Rsr1/Bud1 GTPase involved in selection of a proper growth site in yeast. *J Biol Chem* 277(30):26721–26724.
57. Kozminski KG, et al. (2003) Interaction between a Ras and a Rho GTPase couples selection of a growth site to the development of cell polarity in yeast. *Mol Biol Cell* 14(12):4958–4970.
58. Shimada Y, Wiget P, Gulli MP, Bi E, Peter M (2004) The nucleotide exchange factor Cdc24p may be regulated by auto-inhibition. *EMBO J* 23(5):1051–1062.
59. Zheng Y, Cerione R, Bender A (1994) Control of the yeast bud-site assembly GTPase Cdc42. Catalysis of guanine nucleotide exchange by Cdc24 and stimulation of GTPase activity by Bem3. *J Biol Chem* 269(4):2369–2372.
60. Zheng Y, Bender A, Cerione RA (1995) Interactions among proteins involved in bud-site selection and bud-site assembly in *Saccharomyces cerevisiae*. *J Biol Chem* 270(2): 626–630.
61. Park HO, Bi E (2007) Central roles of small GTPases in the development of cell polarity in yeast and beyond. *Microbiol Mol Biol Rev* 71(1):48–96.
62. Kang PJ, Béven L, Hariharan S, Park HO (2010) The Rsr1/Bud1 GTPase interacts with itself and the Cdc42 GTPase during bud-site selection and polarity establishment in budding yeast. *Mol Biol Cell* 21(17):3007–3016.
63. Chant J, Pringle JR (1995) Patterns of bud-site selection in the yeast *Saccharomyces cerevisiae*. *J Cell Biol* 129(3):751–765.

64. Rupp S, Summers E, Lo HJ, Madhani H, Fink G (1999) MAP kinase and cAMP filamentation signaling pathways converge on the unusually large promoter of the yeast FLO11 gene. *EMBO J* 18(5):1257–1269.
65. Fujita A, et al. (2004) Rax1, a protein required for the establishment of the bipolar budding pattern in yeast. *Gene* 327(2):161–169.
66. Kang PJ, Angerman E, Nakashima K, Pringle JR, Park HO (2004) Interactions among Rax1p, Rax2p, Bud8p, and Bud9p in marking cortical sites for bipolar bud-site selection in yeast. *Mol Biol Cell* 15(11):5145–5157.
67. Chen T, et al. (2000) Multigenerational cortical inheritance of the Rax2 protein in orienting polarity and division in yeast. *Science* 290(5498):1975–1978.
68. Gao XD, et al. (2007) Sequential and distinct roles of the cadherin domain-containing protein Axl2p in cell polarization in yeast cell cycle. *Mol Biol Cell* 18(7): 2542–2560.
69. Caviston JP, Longtine M, Pringle JR, Bi E (2003) The role of Cdc42p GTPase-activating proteins in assembly of the septin ring in yeast. *Mol Biol Cell* 14(10):4051–4066.
70. Pitoniak A, Birkaya B, Dionne HM, Vadaie N, Cullen PJ (2009) The signaling mucins Msb2 and Hkr1 differentially regulate the filamentation mitogen-activated protein kinase pathway and contribute to a multimodal response. *Mol Biol Cell* 20(13): 3101–3114.
71. Reynolds TB, Fink GR (2001) Bakers' yeast, a model for fungal biofilm formation. *Science* 291(5505):878–881.
72. Kron SJ, Styles CA, Fink GR (1994) Symmetric cell division in pseudohyphae of the yeast *Saccharomyces cerevisiae*. *Mol Biol Cell* 5(9):1003–1022.
73. Loeb JD, Kerentseva TA, Pan T, Sepulveda-Becerra M, Liu H (1999) *Saccharomyces cerevisiae* G1 cyclins are differentially involved in invasive and pseudohyphal growth independent of the filamentation mitogen-activated protein kinase pathway. *Genetics* 153(4):1535–1546.
74. Madhani HD, Galitski T, Lander ES, Fink GR (1999) Effectors of a developmental mitogen-activated protein kinase cascade revealed by expression signatures of signaling mutants. *Proc Natl Acad Sci USA* 96(22):12530–12535.
75. Saito H (2010) Regulation of cross-talk in yeast MAPK signaling pathways. *Curr Opin Microbiol* 13(6):677–683.
76. Bardwell L (2006) Mechanisms of MAPK signalling specificity. *Biochem Soc Trans* 34(Pt 5):837–841.
77. Chen RE, Thorner J (2007) Function and regulation in MAPK signaling pathways: Lessons learned from the yeast *Saccharomyces cerevisiae*. *Biochim Biophys Acta* 1773(8):1311–1340.
78. Schwartz MA, Madhani HD (2004) Principles of MAP kinase signaling specificity in *Saccharomyces cerevisiae*. *Annu Rev Genet* 38:725–748.
79. Nern A, Arkowitz RA (2000) G proteins mediate changes in cell shape by stabilizing the axis of polarity. *Mol Cell* 5(5):853–864.
80. Nern A, Arkowitz RA (1999) A Cdc24p-Far1p-Gbetagamma protein complex required for yeast orientation during mating. *J Cell Biol* 144(6):1187–1202.
81. Dyer JM, et al. (2013) Tracking shallow chemical gradients by actin-driven wandering of the polarization site. *Curr Biol* 23(1):32–41.
82. Posas F, et al. (1996) Yeast HOG1 MAP kinase cascade is regulated by a multistep phosphorelay mechanism in the SLN1-YPD1-SSK1 "two-component" osmosensor. *Cell* 86(6):865–875.
83. Westfall PJ, Thorner J (2006) Analysis of mitogen-activated protein kinase signaling specificity in response to hyperosmotic stress: Use of an analog-sensitive HOG1 allele. *Eukaryot Cell* 5(8):1215–1228.
84. Evangelista M, et al. (1997) Bni1p, a yeast formin linking cdc42p and the actin cytoskeleton during polarized morphogenesis. *Science* 276(5309):118–122.
85. Ma XJ, Lu Q, Grunstein M (1996) A search for proteins that interact genetically with histone H3 and H4 amino termini uncovers novel regulators of the Swe1 kinase in *Saccharomyces cerevisiae*. *Genes Dev* 10(11):1327–1340.
86. Chavel CA, Caccamise LM, Li B, Cullen PJ (2014) Global regulation of a differentiation MAPK pathway in yeast. *Genetics* 198(3):1309–1328.
87. Fujita A, et al. (1994) A yeast gene necessary for bud-site selection encodes a protein similar to insulin-degrading enzymes. *Nature* 372(6506):567–570.
88. Adames N, Blundell K, Ashby MN, Boone C (1995) Role of yeast insulin-degrading enzyme homologs in propheromone processing and bud site selection. *Science* 270(5235):464–467.
89. Ni L, Snyder M (2001) A genomic study of the bipolar bud site selection pattern in *Saccharomyces cerevisiae*. *Mol Biol Cell* 12(7):2147–2170.
90. Schenkman LR, Caruso C, Pagé N, Pringle JR (2002) The role of cell cycle-regulated expression in the localization of spatial landmark proteins in yeast. *J Cell Biol* 156(5): 829–841.
91. Chant J, Mischke M, Mitchell E, Herskowitz I, Pringle JR (1995) Role of Bud3p in producing the axial budding pattern of yeast. *J Cell Biol* 129(3):767–778.
92. Adhikari H, Cullen PJ (2015) Role of phosphatidylinositol phosphate signaling in the regulation of the filamentous-growth mitogen-activated protein kinase pathway. *Eukaryot Cell* 14(4):427–440.
93. Caviston JP, Tcheperegine SE, Bi E (2002) Singularity in budding: A role for the evolutionarily conserved small GTPase Cdc42p. *Proc Natl Acad Sci USA* 99(19): 12185–12190.
94. Howell AS, et al. (2009) Singularity in polarization: Rewiring yeast cells to make two buds. *Cell* 139(4):731–743.
95. Wedlich-Soldner R, Altschuler S, Wu L, Li R (2003) Spontaneous cell polarization through actomyosin-based delivery of the Cdc42 GTPase. *Science* 299(5610): 1231–1235.
96. Drees BL, et al. (2001) A protein interaction map for cell polarity development. *J Cell Biol* 154(3):549–571.
97. Harkins HA, et al. (2001) Bud8p and Bud9p, proteins that may mark the sites for bipolar budding in yeast. *Mol Biol Cell* 12(8):2497–2518.
98. Bauer Y, Knechtle P, Wendland J, Helfer H, Philippsen P (2004) A Ras-like GTPase is involved in hyphal growth guidance in the filamentous fungus *Ashbya gossypii*. *Mol Biol Cell* 15(10):4622–4632.
99. Takeshita N, et al. (2013) The cell-end marker TeaA and the microtubule polymerase AlpA contribute to microtubule guidance at the hyphal tip cortex of *Aspergillus nidulans* to provide polarity maintenance. *J Cell Sci* 126(Pt 23):5400–5411.
100. Hausauer DL, Gerami-Nejad M, Kistler-Anderson C, Gale CA (2005) Hyphal guidance and invasive growth in *Candida albicans* require the Ras-like GTPase Rsr1p and its GTPase-activating protein Bud2p. *Eukaryot Cell* 4(7):1273–1286.
101. Valinluck M, Worawatanadharm T, Lu CY, Quintanilla RH, Jr, Banuett F (2014) The cell end marker Tea4 regulates morphogenesis and pathogenicity in the basidiomycete fungus *Ustilago maydis*. *Fungal Genet Biol* 66:54–68.
102. Sabbagh W, Jr, Flatauer LJ, Bardwell AJ, Bardwell L (2001) Specificity of MAP kinase signaling in yeast differentiation involves transient versus sustained MAPK activation. *Mol Cell* 8(3):683–691.
103. DeMarini DJ, et al. (1997) A septin-based hierarchy of proteins required for localized deposition of chitin in the *Saccharomyces cerevisiae* cell wall. *J Cell Biol* 139(1):75–93.

Supporting Information

Basu et al. 10.1073/pnas.1522679113

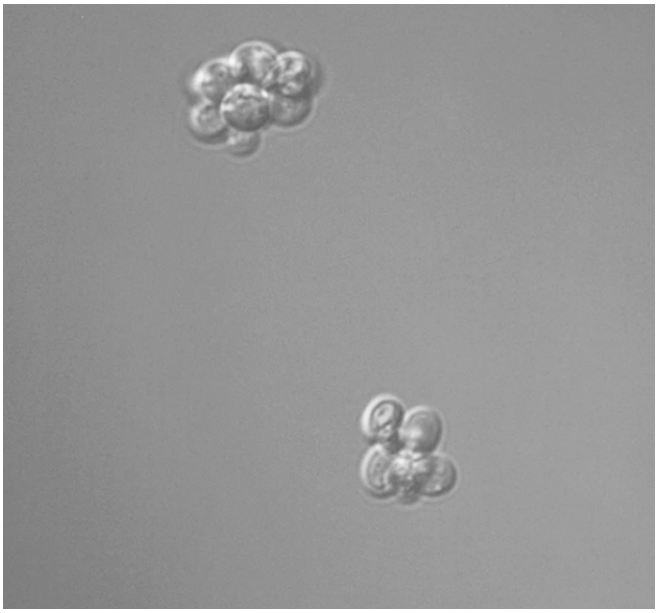

Movie S1. Time-lapse microscopy of cells budding in YEPD medium. The field of view along the *x* axis is ~60 μm.

Movie S1

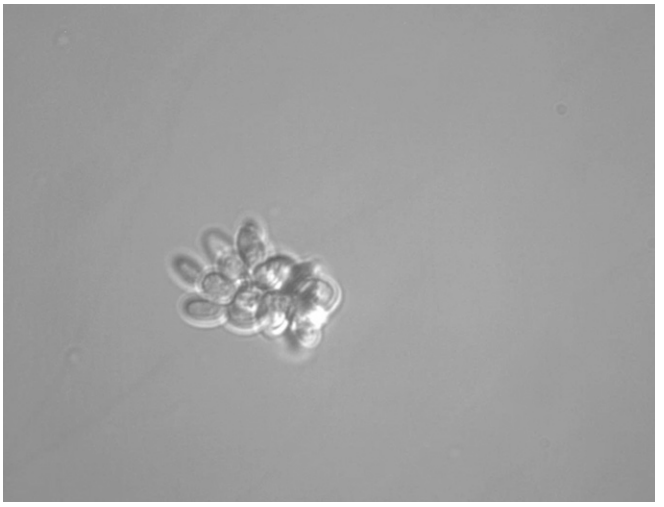

Movie S2. Time-lapse microscopy of cells switched to YEP-Gal medium. The field of view along the *x* axis is ~60 μm.

Movie S2

Other Supporting Information Files

SI Appendix (PDF)

SUPPLEMENTAL DATA

for

Spatial Landmarks Regulate a Cdc42-Dependent MAPK Pathway to Control Differentiation and the Response to Positional Compromise

by Sukanya Basu *, Nadia Vadaie *, Aditi Prabhakar, Boyang Li, Hema Adhikari, Andrew Pitoniak, Jacky Chow, Colin A. Chavel, and Paul J. Cullen†

SUPPLEMENTAL MATERIALS AND METHODS

Microbiological Techniques

Yeast and bacterial strains were grown and manipulated by standard methods (1, 2). For glucose-rich conditions, 2% glucose (Glu; d, dextrose) was used [for yeast extract peptone dextrose (YEPD) or synthetic complete medium containing glucose (SD)]. For low-glucose conditions, 2% galactose (gal) was used (for YEP-Gal or S-Gal). In some cases, 0.2% glu was used as indicated. All experiments were carried out at 30˚C unless otherwise indicated. The single cell invasive growth assay (3) and the plate-washing assay (4) have been described. ß-galactosidase assays were performed as described (5). Values represent the average of at least two independent trials and are expressed in Miller units. P-values were calculated by a two-tailed students' t test. *FUS1-HIS3* expression [the *FUS1* promoter linked to the *HIS3* coding sequence (6)] was measured by spotting equal concentrations of cells onto SD-HIS medium or SD-HIS with 3-Amino-1,2,4-triazole (3-AT). Halo assays were performed as described (7). Assays to evaluate the role of Rsr1p in the HOG pathway were performed as described (8, 9). Spot plate and

invasive growth assay plate images were manipulated using the invert function on Photoshop to visualize spotted cells and invasive scars.

Strains and Plasmids

Yeast strains are listed in Table S1. Plasmids are listed in Table S2. Overexpression constructs were obtained from an ordered collection obtained from Open Biosystems (10). Gene disruptions and *GAL1* promoter fusions were made by PCR-based methods (11, 12). A subset of gene deletions were constructed with antibiotic resistance markers on cassettes *NAT* (PC2205) and *HYG* (PC2206) (13). Gene disruptions were confirmed by PCR Southern analysis and phenotype. To generate the Bud3p-mCherry fusion (PC6533), a PCR product was generated with primers designed to create an in frame fusion between the C-terminus of the *BUD3* ORF and mCherry using pFA6a-*mCherry-kanMX6* (14) as a template, which was provided by the yeast resource center (http://depts.washington.edu/yeastrc/). The PCR product was transformed into wild-type cells (PC1024). PC6533 was transformed with pGFP-Bud8p for co-localization experiments.

Plasmids pRS315 and pRS316 have been described (15). pRS316-CDC24 GFP was provided by Rong Li. Plasmids pRS426 *AXL2 (#235) 1-823* (PC4146), pRS426 *AXL2 (#238) p1-646* (PC4147), pRS426 *AXL2 (#319) p1-544* (PC4149)*, 641-725* (PC4149), pRS426 *AXL2 (#320) p1-544, 641-685* (PC4150), pRS426 *AXL2 (#318) p1-544, 726-823* (PC4151) described in (16) were provided by Erfei Bi (University of Pennsylvania, Philadelphia, PA).

Plasmids carrying YEplac195-*RSR1* (pHP1118) (17), YEp1ac195-*rsr1*^{T35A} (pHP1124) (17), YEp13-*RSR1* (pHP562, YEp13-*rsr1*^{K16N} (pHP596) (18), YEp13-*rsr1*^{G12V} (pHP595) (18), YEplac195-rsr1-7$^{K260-264S}$(pHP1123) (17),YEplac195-*rsr1*-8K$^{260-261S}$(pHP1755) (19), and YEplac195-*rsr1*-9K$^{263-264S}$ (pHP1753) (19) were provided by Hay-Oak Park (Ohio State University, Columbus OH). YEpGFP-Bud8p (PC1883) was provided by John Pringle (Stanford University, Palo Alto, CA). pAXL1-HA (p151) was provided by C. Boone (20). Plasmid p*FRE-lacZ* (PC1405) was provided by Hiten Madhani (21).

Phosphoblot analysis

Immunoblots were performed as described (22). Proteins were separated by SDS-PAGE on 10% acrylamide gels and transferred to nitrocellulose membranes (protran BA85, VWR International Inc. Bridgeport NJ). Membranes were incubated in blocking buffer (5% nonfat dry milk, 10mM Tris-HCl pH8, 150mM NaCl and 0.05% Tween 20) for 1 h at 25˚C. Western Bright kit from Advansta Inc. (Menlo Park, CA; LPS #K-12045-D20) or ECL Plus immunoblotting reagents were used to detect secondary antibodies (Amersham Biosciences, Piscataway NJ). Nitrocellulose membranes were incubated for 18 h at 4˚C in blocking buffer.

Phosphoblot analysis was performed according to established protocols (23, 24) and adapted to the lab as described (7) with the following changes. Samples were processed immediately. To detect phosphorylated Kss1p, p42/p44 antibodies (Cell Signaling Technology, Danvers, MA; #4370) were diluted in 1:5000 in blocking buffer and incubated 16 hrs at 4°C. Kss1p was detected by using anti-Kss1p antibodies (Santa

Cruz Biotechnology, Santa Cruz, CA; #6775) diluted to 1:5000 in blocking buffer. Total protein level was estimated by anti Pgk1p antibody in 1:10,000 (Life Technologies; Camarillo, CA; #459250). Phospho p38 antibodies were used to detect P~Hog1p (Cell Signaling Technologies Danvers MA #9211), and total Hog1p was detected using anti-Hog1p antibodies (Santa Cruz Biotechnology, Santa Cruz CA; #yC-20). For secondary antibodies (goat anti-mouse IgG–HRP, Bio-Rad Laboratories, Hercules, CA; #170-6516; goat anti-rabbit IgG-HRP, Jackson ImmunoResearch Laboratories, Inc., West Grove, PA; #111-035-144; and donkey anti-goat IgG-HRP Santa Cruz Biotechnology, Santa Cruz, CA; #sc-2020) were used according to manufacturer's protocols. Quantitation of band intensities for immunoblot analysis was performed with Image Lab Software (Bio-Rad, Inc.). Band intensities were determined for phosphoproteins relative to Kss1p or Hog1p levels, which was set to 1 for wild-type samples and adjusted for other samples accordingly.

qPCR Analysis

Quantitative polymerase chain reaction (qPCR) experiments and analysis were performed according to established protocols (25, 26). Cells were harvested from 10 ml cultures in YEPD or YEP-Gal medium for 5.5 h. RNA was isolated by hot acid phenol extraction. RNA concentration was measured using nanodrop 2000c spectrophotometer (Thermo Fisher scientific, Wilmington, USA). One microgram of total RNA was used for cDNA synthesis using iScript cDNA synthesis kit (Bio-Rad Herculase, CA) synthesis Kit according to the manufacturer's protocol. One third of the total DNA was used for real time qPCR in 25 µl reaction using Biorad iQ5 optical system cycler (Bio-Rad, Herculase,

CA). Amplification cycle, melt curve and gene quantification was performed as described (25, 27) using SYBR green supermix (Biorad Hercules, CA USA). Primer sequences were based on previous report (28). For the *FLO11* gene the primer sequences are forward 5'-GTTCAACCAGTCCAAGCGAAA-3'and reverse 5'-GTAGTTACAGGTGTGGTAGGTGAAGTG-3'. For *ACT1,* forward 5'-GGCTTCTTTGACTACCTTCCAACA-3' and reverse 5'-GATGGACCACTTTCGTCGTATTC-3' primers were used. The *ACT1* gene was used as an internal control for total input RNA levels. At least two independent biological replicates were performed. Average values are reported. P-values were calculated using 2 sample student t-test with equal variance probability from delta CT values using minitab17 statistical software package (Minitab Inc. 2010 State college PA, USA).

Budding Pattern Analysis

Budding pattern was determined as described (29). Budding pattern was determined by bud position and the assignment of bud scar position to the proximal, equatorial, or distal regions of the cell. Cells in mid-log phase were resuspended in 1ml of water, and stained with Calcofluor White Fluorescent brightener 28 (CFW) (Sigma-Aldrich Life Science and Biochemicals, St. Louis, MO) to a final concentration of 0.01% for 10 min, at 25˚C. Cells were washed once in water and examined by microscopy. Budding pattern analysis agreed closely with the two-fluorescent staining approach (25).

Two-fluorescence staining was based on established techniques (30, 31). For FITC-Concanavalin A (ConA) (Sigma-Aldrich) and TRITC-ConA (Sigma-Aldrich) labeling experiments, cells were grown in YEPD medium for 16 hrs. Cells were sub-

cultured in YEPD for 2h 40 min, and FITC-ConA was added to a final concentration of 0.1mg/ml. Cells were incubated for 20 min at 30°C, harvested by centrifugation and washed 3 times in distilled water. Cells were resuspended in YEP-Gal medium and incubated for the indicated time periods. TRITC-ConA was added to a final concentration of 0.1mg/ml, and cells were incubated for 20 min. Cells were harvested by centrifugation, washed 3 times in distilled water and visualized by fluorescence microcopy.

ConA binds to α-mannosyl and α-glucosyl oligosaccharides (32). Staining of cells by FITC-ConA and TRITC-ConA in YEP-Gal medium was not effective possibly due to altered glycosylation of the cell wall during growth in gal (33). To evaluate cells switching from YEP-Gal to YEPD medium, CFW was used. For CFW labeling, 1% (w/v) CFW stock solution was made fresh. Cells were grown in YEP-Gal medium for 16h and sub-cultured in YEP-Gal medium for 3 hrs. CFW was added to a final concentration of 0.002% (w/v), and cells were incubated for 5 min. Cells were harvested by centrifugation, washed 3 times in distilled water and resuspended in YEPD medium for the indicated time periods. FITC-ConA was added to a final concentration of 0.1mg/ml for 20 min. Cells were harvested by centrifugation, washed 3 times in distilled water and visualized by fluorescence microcopy. For the switchback experiment, cells were sub-cultured in YEPD medium for 3 hrs, harvested by centrifugation, washed 3 times in water and resuspended in YEP-Gal medium. Cells were examined every hour by microscopy. After 3 hr in YEP-Gal, cells were split into YEP-Gal for 3 additional hrs, or harvested by centrifugation, washed 3 times in distilled water and resuspended in YEPD medium for 3h. Each experiment was performed in duplicate. More than 80 cells were counted in each trial.

Evaluating Budding Pattern by Time Lapse Microscopy

To evaluate the switch to distal-pole budding upon glucose limitation, cells were grown to mid-log phase in YEPD media, washed and resuspended in YEP-Gal and incubated at 30˚C. Cells were removed and assessed for budding pattern over time. For time-lapse microscopy, slides with wells (MP Biomedicals LLC 096041205) were coated with 0.1 mg/ml polylysine (Chemicon CAT A-003-E). Slides were dried at 25˚C and washed six times with distilled water. Cells were grown to saturation in YEPD and sub-cultured to mid-log phase for 3 hrs in fresh medium (YEPD or YEP-Gal) at 30°C. One drop of cell suspension (approximately 3-5 µl) was placed on slides. After settling (approximately 5 minutes), excess media and floating cells were aspirated by micropipette, and pre-warmed media at 30°C was added to the wells. Wells were covered with coverslips and examined by DIC over time.

To evaluate the switch back to axial budding upon glucose addition, the single cell time course experiment was performed (3). Cells were spread onto S-Glu media and incubated for 16 hrs at 30˚C. The plate was examined at 20X at time zero. A spot of 6% glucose was added in a 300 µl aliquot to the plate in an area surrounding the photographed cells. After the liquid had evaporated, the plate was returned to 30˚C. At specific time points, the plate was removed from 30˚C, and cells were photographed in multiple focal planes in the Z-axis at 20X. At the final time point, a coverslip was added to the spot, and cells were examined at 100X at multiple focal planes. For bud assignment during the single cell time course, buds were considered axial (proximal) if they could be directly observed emerging from a daughter cell at any focal plane or if two equal sized

buds were seen emerging from a mother-daughter pair. As a control, cells were examined over time without a spot of glucose added.

Microscopy

Differential-interference-contrast (DIC) and fluorescence microscopy of the GFP protein using FITC filter sets were performed using an Axioplan 2 fluorescent microscope (Zeiss) with a PLAN-APOCHROMAT 100X/1.4 (oil) objective (N.A. 0.17)(Zeiss). For most experiments, proteins were visualized by resuspending cells in water at 25˚C. Digital images were obtained with the Axiocam MRm camera (Zeiss). Axiovision 4.4 software (Zeiss) was used for image acquisition and analysis.

Electron microscopy was based on established protocols (34). For electron micrographs, cells were grown overnight in YEPD medium. 2ul of A600=0.02 cells were spotted onto 35um microsieves (BioDesign Inc. of New York, Cat#N35S) laid on YEPGal and allowed to grow for 16 hrs. Sieves were transferred to petri dishes for fixation (2% glutaraldehyde for 4h at 4C) and dehydration (30%, 50%, 70%, 85%, 95% ethanol for 15 mins, and twice in 100% ethanol for 15 min). Samples were critical point dried in hexamethyldisilazane for 16 hrs. Samples were carbon coated and imaged on a Hitachi S4000 Field Emission Scanning Electron Microscope (FESEM).

REFERENCES

1. Sambrook J, Fritsch, E.F., and Maniatis, T. (1989) Molecular cloning: a laboratory manual. *Cold Spring Harbor Laboratory Press, Cold Spring Harbor, NY.*
2. Rose MD, Winston, F., and Hieter, P. (1990) Methods in yeast genetics. *Cold Spring Harbor Laboratory Press, Cold Spring Harbor, NY.*

3. Cullen PJ & Sprague GF, Jr. (2000) Glucose depletion causes haploid invasive growth in yeast. *Proceedings of the National Academy of Sciences of the United States of America* 97(25):13619-13624.
4. Roberts RL & Fink GR (1994) Elements of a single MAP kinase cascade in Saccharomyces cerevisiae mediate two developmental programs in the same cell type: mating and invasive growth. *Genes & development* 8(24):2974-2985.
5. Cullen PJ*, et al.* (2000) Defects in protein glycosylation cause SHO1-dependent activation of a STE12 signaling pathway in yeast. *Genetics* 155(3):1005-1018.
6. Horecka J & Sprague GF, Jr. (1996) Identification and characterization of FAR3, a gene required for pheromone-mediated G1 arrest in Saccharomyces cerevisiae. *Genetics* 144(3):905-921.
7. Pitoniak A*, et al.* (2015) Cdc42p-interacting protein bem4p regulates the filamentous-growth mitogen-activated protein kinase pathway. *Molecular and cellular biology* 35(2):417-436.
8. Adhikari H & Cullen PJ (2014) Metabolic Respiration Induces AMPK- and Ire1p-Dependent Activation of the p38-Type HOG MAPK Pathway. *PLoS genetics* 10(10):e1004734.
9. Posas F & Saito H (1998) Activation of the yeast SSK2 MAP kinase kinase kinase by the SSK1 two-component response regulator. *The EMBO journal* 17(5):1385-1394.
10. Gelperin DM*, et al.* (2005) Biochemical and genetic analysis of the yeast proteome with a movable ORF collection. *Genes & development* 19(23):2816-2826.
11. Baudin A, Ozier-Kalogeropoulos O, Denouel A, Lacroute F, & Cullin C (1993) A simple and efficient method for direct gene deletion in Saccharomyces cerevisiae. *Nucleic Acids Res* 21(14):3329-3330.
12. Longtine MS*, et al.* (1998) Additional modules for versatile and economical PCR-based gene deletion and modification in Saccharomyces cerevisiae. *Yeast* 14(10):953-961.
13. Goldstein AL & McCusker JH (1999) Three new dominant drug resistance cassettes for gene disruption in Saccharomyces cerevisiae. *Yeast* 15(14):1541-1553.
14. Shaner NC*, et al.* (2004) Improved monomeric red, orange and yellow fluorescent proteins derived from Discosoma sp. red fluorescent protein. *Nature biotechnology* 22(12):1567-1572.
15. Sikorski RS & Hieter P (1989) A system of shuttle vectors and yeast host strains designed for efficient manipulation of DNA in Saccharomyces cerevisiae. *Genetics* 122(1):19-27.
16. Gao XD*, et al.* (2007) Sequential and distinct roles of the cadherin domain-containing protein Axl2p in cell polarization in yeast cell cycle. *Molecular biology of the cell* 18(7):2542-2560.
17. Kozminski KG*, et al.* (2003) Interaction between a Ras and a Rho GTPase couples selection of a growth site to the development of cell polarity in yeast. *Molecular biology of the cell* 14(12):4958-4970.
18. Ruggieri R*, et al.* (1992) RSR1, a ras-like gene homologous to Krev-1 (smg21A/rap1A): role in the development of cell polarity and interactions with

the Ras pathway in Saccharomyces cerevisiae. *Molecular and cellular biology* 12(2):758-766.
19. Kang PJ, Beven L, Hariharan S, & Park HO (2010) The Rsr1/Bud1 GTPase interacts with itself and the Cdc42 GTPase during bud-site selection and polarity establishment in budding yeast. *Molecular biology of the cell* 21(17):3007-3016.
20. Adames N, Blundell K, Ashby MN, & Boone C (1995) Role of yeast insulin-degrading enzyme homologs in propheromone processing and bud site selection. *Science* 270(5235):464-467.
21. Madhani HD, Styles CA, & Fink GR (1997) MAP kinases with distinct inhibitory functions impart signaling specificity during yeast differentiation. *Cell* 91(5):673-684.
22. Vadaie N*, et al.* (2008) Cleavage of the signaling mucin Msb2 by the aspartyl protease Yps1 is required for MAPK activation in yeast. *The Journal of cell biology* 181(7):1073-1081.
23. Lee MJ & Dohlman HG (2008) Coactivation of G protein signaling by cell-surface receptors and an intracellular exchange factor. *Current biology : CB* 18(3):211-215.
24. Sabbagh W, Jr., Flatauer LJ, Bardwell AJ, & Bardwell L (2001) Specificity of MAP kinase signaling in yeast differentiation involves transient versus sustained MAPK activation. *Molecular cell* 8(3):683-691.
25. Chavel CA, Caccamise LM, Li B, & Cullen PJ (2014) Global regulation of a differentiation MAPK pathway in yeast. *Genetics* 198(3):1309-1328.
26. Pfaffl MW (2001) A new mathematical model for relative quantification in real-time RT-PCR. *Nucleic Acids Res* 29(9):e45.
27. Livak KJ & Schmittgen TD (2001) Analysis of relative gene expression data using real-time quantitative PCR and the 2(-Delta Delta C(T)) Method. *Methods* 25(4):402-408.
28. Chavel CA, Dionne HM, Birkaya B, Joshi J, & Cullen PJ (2010) Multiple signals converge on a differentiation MAPK pathway. *PLoS genetics* 6(3):e1000883.
29. Chant J & Pringle JR (1995) Patterns of bud-site selection in the yeast Saccharomyces cerevisiae. *The Journal of cell biology* 129(3):751-765.
30. Nern A & Arkowitz RA (2000) G proteins mediate changes in cell shape by stabilizing the axis of polarity. *Molecular cell* 5(5):853-864.
31. Matheos D, Metodiev M, Muller E, Stone D, & Rose MD (2004) Pheromone-induced polarization is dependent on the Fus3p MAPK acting through the formin Bni1p. *The Journal of cell biology* 165(1):99-109.
32. Lis H & Sharon N (1998) Lectins: Carbohydrate-Specific Proteins That Mediate Cellular Recognition. *Chemical reviews* 98(2):637-674.
33. Adhikari H*, et al.* (2015) Role of the unfolded protein response in regulating the mucin-dependent filamentous-growth mitogen-activated protein kinase pathway. *Molecular and cellular biology* 35(8):1414-1432.
34. Piccirillo S & Honigberg SM (2011) Yeast colony embedding method. *Journal of visualized experiments : JoVE* (49).
35. Cullen PJ & Sprague GF, Jr. (2002) The roles of bud-site-selection proteins during haploid invasive growth in yeast. *Molecular biology of the cell* 13(9):2990-3004.

36. Chant J & Herskowitz I (1991) Genetic control of bud site selection in yeast by a set of gene products that constitute a morphogenetic pathway. *Cell* 65(7):1203-1212.
37. Roemer T, Madden K, Chang J, & Snyder M (1996) Selection of axial growth sites in yeast requires Axl2p, a novel plasma membrane glycoprotein. *Genes & development* 10(7):777-793.
38. Fujita A*, et al.* (1994) A yeast gene necessary for bud-site selection encodes a protein similar to insulin-degrading enzymes. *Nature* 372(6506):567-570.
39. Chant J, Corrado K, Pringle JR, & Herskowitz I (1991) Yeast BUD5, encoding a putative GDP-GTP exchange factor, is necessary for bud site selection and interacts with bud formation gene BEM1. *Cell* 65(7):1213-1224.
40. Park HO, Chant J, & Herskowitz I (1993) BUD2 encodes a GTPase-activating protein for Bud1/Rsr1 necessary for proper bud-site selection in yeast. *Nature* 365(6443):269-274.
41. Zahner JE, Harkins HA, & Pringle JR (1996) Genetic analysis of the bipolar pattern of bud site selection in the yeast Saccharomyces cerevisiae. *Molecular and cellular biology* 16(4):1857-1870.
42. Ni L & Snyder M (2001) A genomic study of the bipolar bud site selection pattern in Saccharomyces cerevisiae. *Molecular biology of the cell* 12(7):2147-2170.
43. Lord M*, et al.* (2002) Subcellular localization of Axl1, the cell type-specific regulator of polarity. *Current biology : CB* 12(15):1347-1352.
44. Fujita A*, et al.* (2004) Rax1, a protein required for the establishment of the bipolar budding pattern in yeast. *Gene* 327(2):161-169.
45. Chen T*, et al.* (2000) Multigenerational cortical inheritance of the Rax2 protein in orienting polarity and division in yeast. *Science* 290(5498):1975-1978.
46. Adhikari H*, et al.* (2015) Role of the Unfolded Protein Response In Regulating the Mucin-Dependent Filamentous Growth MAPK Pathway. *Molecular and cellular biology*.
47. Liu H, Styles CA, & Fink GR (1993) Elements of the yeast pheromone response pathway required for filamentous growth of diploids. *Science* 262(5140):1741-1744.
48. Cullen PJ*, et al.* (2004) A signaling mucin at the head of the Cdc42- and MAPK-dependent filamentous growth pathway in yeast. *Genes & development* 18(14):1695-1708.
49. Bender A & Pringle JR (1992) A Ser/Thr-rich multicopy suppressor of a cdc24 bud emergence defect. *Yeast* 8(4):315-323.
50. Richman TJ & Johnson DI (2000) Saccharomyces cerevisiae cdc42p GTPase is involved in preventing the recurrence of bud emergence during the cell cycle. *Molecular and cellular biology* 20(22):8548-8559.
51. Pitoniak A, Birkaya B, Dionne HM, Vadaie N, & Cullen PJ (2009) The signaling mucins Msb2 and Hkr1 differentially regulate the filamentation mitogen-activated protein kinase pathway and contribute to a multimodal response. *Molecular biology of the cell* 20(13):3101-3114.
52. Adhikari H & Cullen PJ (2015) Role of phosphatidylinositol phosphate signaling in the regulation of the filamentous-growth mitogen-activated protein kinase pathway. *Eukaryotic cell* 14(4):427-440.

53. Siliciano PG & Tatchell K (1984) Transcription and regulatory signals at the mating type locus in yeast. *Cell* 37(3):969-978.
54. Madhani HD & Fink GR (1997) Combinatorial control required for the specificity of yeast MAPK signaling. *Science* 275(5304):1314-1317.
55. Stevenson BJ, Rhodes N, Errede B, & Sprague GF, Jr. (1992) Constitutive mutants of the protein kinase STE11 activate the yeast pheromone response pathway in the absence of the G protein. *Genes & development* 6(7):1293-1304.
56. Marles JA, Dahesh S, Haynes J, Andrews BJ, & Davidson AR (2004) Protein-protein interaction affinity plays a crucial role in controlling the Sho1p-mediated signal transduction pathway in yeast. *Molecular cell* 14(6):813-823.
57. Schenkman LR, Caruso C, Page N, & Pringle JR (2002) The role of cell cycle-regulated expression in the localization of spatial landmark proteins in yeast. *The Journal of cell biology* 156(5):829-841.
58. Caviston JP, Tcheperegine SE, & Bi E (2002) Singularity in budding: a role for the evolutionarily conserved small GTPase Cdc42p. *Proceedings of the National Academy of Sciences of the United States of America* 99(19):12185-12190.
59. Wai SC, Gerber SA, & Li R (2009) Multisite phosphorylation of the guanine nucleotide exchange factor Cdc24 during yeast cell polarization. *PloS one* 4(8):e6563.
60. Sheu YJ, Barral Y, & Snyder M (2000) Polarized growth controls cell shape and bipolar bud site selection in Saccharomyces cerevisiae. *Molecular and cellular biology* 20(14):5235-5247.
61. Michelitch M & Chant J (1996) A mechanism of Bud1p GTPase action suggested by mutational analysis and immunolocalization. *Current biology : CB* 6(4):446-454.
62. Tong Z*, et al.* (2007) Adjacent positioning of cellular structures enabled by a Cdc42 GTPase-activating protein-mediated zone of inhibition. *The Journal of cell biology* 179(7):1375-1384.

SUPPLEMENTAL FIGURE LEGENDS

Figure S1. Role of Rsr1p in regulating fMAPK by the *FUS1-HIS3* reporter. A) *FRE-lacZ* analysis of the *rsr1*Δ mutant in basal and inducing conditions alongside controls. ß-galactosidase assays were performed as described in Fig. 1C. **B)** Serial dilutions of cells at the same starting concentration were spotted onto SD + amino acids (AA) or SD-HIS (histidine) media. Strains are ∑1278b *ste4* and contain an integrated version of *FUS1-HIS3*. **C)** *FUS1-HIS3* activity in the *pmi40-101 rsr1*Δ mutant compared to wild-type cells and the *ste12*Δ mutant. All strains are *ste4 pmi40-101 FUS1-HIS3.* Equal concentrations of cells were spotted onto media containing 50 mM mannose (Man), which suppresses the glycosylation defect of the *pmi40-101* mutant (5). **D)** P~Kss1p levels were examined as in Fig. 1A in the *cdc24::NAT* and *cdc24::NAT bud4*Δ strains carrying the YEp351-*MYR-Cdc24p-GFP* (Myr-Cdc24p) plasmids alongside controls.

Figure S2. Activity of fMAPK in bud-site-selection mutants. A) P~Kss1p analysis of *bud*Δ mutants alongside controls. P~Kss1p levels were examined as in Fig. 1A. **B)** Equal concentrations of cells were spotted onto SD+AA and SD-HIS media for 3 days at 30°C. At right, typical budding patterns of the indicated mutants, verified for these strains in (35), is shown. The + sign refers to >90% axial pattern. Strains are ∑1278b *ste4 FUS1-HIS3.* Bud3p, Bud4p, Axl2p/Bud10p (36, 37)], Axl1p (20, 38), Rsr1p, the GEF Bud5p (39), the GAP Bud2p (40) and Bud7p (41, 42) have been described. **C)** Expression of *FUS1-lacZ* in the indicated mutants (all mutants are ∑1278b *ste4 FUS1-HIS3*). ß-galactosidase assays were performed from cell extracts derived from mid-log phase cells

grown for 5.5 hrs in YEPD media. ß-galactosidase assays were performed as described in Fig. 1C.

Figure S3. Activity of fMAPK in *rax* mutants. A) P~Kss1p analysis of *rax1*Δ and *rax2*Δ mutants alongside controls. P~Kss1p levels were examined as in Fig. 1A. **B)** P~Kss1p analysis of *rax* and indicated axial bud site mutant combinations alongside controls. P~Kss1p levels were examined as in Fig. 1A. **C)** The indicated mutant combinations with *rax1*Δ were spotted onto SD+AA and SD-HIS media. Rax1p and Rax2p roles in bud-site-selection have been described (43-45). **D)** Expression of *FUS1-lacZ* in the indicated mutants (all mutants are ∑1278b *ste4 FUS1-HIS3*). ß-galactosidase assays were performed as described in Fig. 1C. **E)** Invasive growth of the *rax1*Δ and *rax2*Δ mutants and control strains in YEP-GAL media. **F)** Budding pattern of the *rax1*Δ and *rax2*Δ mutants and control strains in YEP-GAL media. Asterisk, p value <0.05. Budding at the axial (A), equatorial (E), or distal poles (D) were assessed.

Figure S4. Evaluation of an *AXL2* deletion series and the role of Axl1p in the fMAPK response to protein glycosylation deficiency. A) P~Kss1p levels in Axl2p truncation mutants defective for axial budding, and/or suppression of *cdc42*^{V36G} as indicated by the +/- signs (16). P~Kss1p levels were examined as in Fig. 1A. ND, not determined. **B)** Cells containing the indicated plasmids were spotted on SD-URA to select for plasmids. WT, wild-type cells carrying pRS316. The *axl2Δ* mutant also carries pRS316. The axial budding pattern and *cdc42*^{V36G} suppression has been reported (16). Integrative (pRS306-based) plasmids containing equivalent *AXL2* deletions from (16)

gave equivalent results. **C)** *FUS1-HIS3* activity in four independent *axl1*Δ mutants compared to the *pmi40-101* and *pmi40-101 ste12*Δ mutant. Cells were also spotted onto SD-HIS + 3-AT to evaluate *HIS3* activity. Strains are ∑1278b *ste4 FUS1-HIS3*. **D)** P~Kss1p levels were examined as in Fig. 1A for the strains indicated (YEP-GAL).

Figure S5. Role of the Msb2p- and Rsr1p- branches in regulating fMAPK pathway. **A)** *FUS1-HIS3* activity in the *msb2*Δ and *rsr1*Δ single mutants and the *msb2*Δ *rsr1*Δ double mutant at 1 day. **B)** Suppression of the fMAPK defect of *rsr1*Δ by Msb2p$^{\Delta 100\text{-}818}$. **C)** Suppression of the fMAPK defect of *rsr1*Δ by pGFP-MSB2 [another hyperactive version of Msb2 (46)] and pSHO1^{P120L}. **D)** P~Kss1p analysis of hyperactive fMAPK alleles in the *axl2*Δ mutant. P~Kss1p levels were examined as in Fig. 1A. **E)** Suppression of the invasive growth defect and *FUS1-HIS3* activity of the *axl2*Δ mutant by Msb2p$^{\Delta 100\text{-}818}$. Equal concentrations of cells were spotted onto the indicated media. Soft wash refers to washing cells off the plate with a gentle stream of water. Hard wash requires rubbing cells off of the plate by hand. All strains are ∑1278b *ste4 FUS1-HIS3*.

Figure S6. Role of Rsr1p in regulating the mating and the HOG pathways. A) Wild-type cells and the *rsr1*Δ mutant were grown to mid-log phase in YEPD, treated with 5μM pheromone for 30 min, and evaluated for P~Fus3p levels by immunoblot analysis. The experiment was performed in triplicate. Average values are shown. NS, no significant difference was detected. **B)** Activity of the *FUS1-lacZ* reporter in the indicated strains. Cells were grown to mid-log phase in YEPD. ß-galactosidase assays were performed as

described in Fig. 1C. **C)** P~Kss1p analysis of polarized growth mutants. P~Kss1p levels were examined as in Fig. 1A.

Figure S7. Analysis of budding pattern of haploid cells in different nutrient conditions over time. Examples of wild-type (PC538) and *ste12*Δ (PC539) cells grown in YEPD and shifted to YEPD or YEP-Gal for the indicated times. Dots refer to distal-unipolar buds. Bar, 20 μm.

Figure S8. Evaluation of budding pattern changes in response to changes in glucose levels. Examples of the budding pattern switch of wild-type (PC538) cells undergoing filamentous growth after addition of exogenous glucose by the single cell invasive growth assay. Cells were spread on S-Glu for 12 h and examined at the indicated time points after glucose addition. Bar, 30 microns.

Figure S9. Regulation of glucose-dependent changes in budding pattern. Two-fluorescence microscopy of cells carrying GFP-Bud8p and Bud3p-mCherry. Black arrows refer to the site where budding is expected to occur for daughter cells, based on observations of cells under equivalent growth conditions. White arrows refer to marks not utilized under the condition tested.

Supplemental Movie 1. Time-lapse microscopy of cells budding in YEPD medium.

Supplemental Movie 2. Time-lapse microscopy of cells switched to YEP-Gal medium.

SUPPLEMENTAL TABLES

Table S1. Yeast Strains.

Name	Genotype [a]	Reference
PC1291[b]	*MATα ste4 FUS1-HIS3 ura3-52*	(5)
PC244 [b]	*MATα ste4 FUS1-HIS3 ura3-52 pmi40-101*	(5)
PC313	*MAT***a** *ura3-52*	(47)
PC344	*MAT***a** *ura3-52 / MATα ura3-52*	(3)
PC424 [b]	*MATα ste4 FUS1-HIS3 ura3-52 pmi40-101 ste20::URA3*	(5)
PC538	*MAT***a** *ste4 FUS1-lacZ FUS1-HIS3 ura3-52*	(48)
PC539	*MAT***a** *ste4 FUS1-lacZ FUS1-HIS3 ura3-52 ste12::URA3*	(48)
PC471	*MAT***a** *ste4 FUS1-lacZ FUS1-HIS3 ura3-52 bud6::URA3*	(35)
PC544	*MAT***a** *ste4 FUS1-lacZ FUS1-HIS3 ura3-52 bni1::URA3*	(35)
PC551	*MAT***a** *ste4 FUS1-lacZ FUS1-HIS3 ura3-52 pea2::URA3*	(35)
PC552	*MAT***a** *ste4 FUS1-lacZ FUS1-HIS3 ura3-52 hsl1::URA3*	(5)
PC554	*MAT***a** *ste4 FUS1-lacZ FUS1-HIS3 ura3-52 spa2::URA3*	(35)
PC555	*MAT***a** *ste4 FUS1-lacZ FUS1-HIS3 ura3-52 hsl7::URA3*	(5)
PC563	*MAT***a** *ste4 FUS1-lacZ FUS1-HIS3 ura3-52 bud8::KlURA3*	(35)
PC611	*MAT***a** *ste4 FUS1-lacZ FUS1-HIS3 ura3-52 ste11::URA3*	This study
PC617	*MAT***a** *ste4 FUS1-lacZ FUS1-HIS3 ura3-52 bud7::KlURA3*	(35)
PC618	*MAT***a** *ste4 FUS1-lacZ FUS1-HIS3 ura3-52 axl2::KlURA3*	(48)
PC622	*MAT***a** *ste4 FUS1-lacZ FUS1-HIS3 ura3-52 GAL-SHO1::KanMX6*	(48)
PC637	*MAT***a** *ste4 FUS1-lacZ FUS1-HIS3 ura3-52 bud4::KlURA3*	(35)
PC638	*MAT***a** *ste4 FUS1-lacZ FUS1-HIS3 ura3-52 bud5::KlURA3*	(35)
PC639	*MAT***a** *ste4 FUS1-lacZ FUS1-HIS3 ura3-52 axl1*	(35)
PC642	*MAT***a** *ste4 FUS1-lacZ FUS1-HIS3 ura3-52 pbs2::ura3- sho1::KlURA3* [c]	This study
PC643	*MAT***a** *ste4 FUS1-lacZ FUS1-HIS3 ura3-52 pbs2::ura3- ste20::URA3*	This study
PC644	*MAT***a** *ste4 FUS1-lacZ FUS1-HIS3 ura3-52 pbs2::ura3- ste12::URA3*	This study
PC646	*MAT***a** *ste4 FUS1-lacZ FUS1-HIS3 ura3-52 pbs2::ura3-*	This study
PC652	*MATα ura3-52 his3::ura3-*	(35)
PC776	*MAT***a** *ste4 FUS1-lacZ FUS1-HIS3 ura3-52 rsr1::HIS3*	(35)
PC780	*MAT***a** *ura3-52 his3 axl1::CgHIS3* [d]	(35)
PC781	*MATα ura3-52 his3 bud7::CgHIS3* [d]	(35)
PC782	*MATα ura3-52 his3 bud8::CgHIS3* [d]	(35)
PC787	*MAT***a** *ura3-52 GAL-AXL1::KanMX6*	(35)
PC859	*MATα ura3-52 ura3- his3*	(35)
PC860	*MATα ura3-52 ura3- his3 bud2::HIS3*	(35)
PC948	*MAT***a** *ste4 FUS1-lacZ FUS1-HIS3 ura3-52 msb2::KanMX6*	(48)
PC1019	*MAT***a** *ste4 FUS1-lacZ FUS1-HIS3 ura3-52 pbs2::URA3*	This study
PC1020	*MAT***a** *ste4 FUS1-lacZ FUS1-HIS3 ura3-52 pbs2::URA3 msb2::KanMX6*	This study
PC1024	*MAT***a** *ste4 FUS1-HIS3 FUS1-LacZ ura3-52 leu2::URA3*	This study
PC1436	*MAT***a** *cdc24-4 ura3 leu2 his3*	(49)
PC1437	*MATα cdc42-1 ura3 leu2 his3 trp1*	(50)
PC1516	*MAT***a** *ste4 FUS1-lacZ FUS1-HIS3 ura3-52 MSB2-HAΔ100–818*	(48)
PC1523	*MAT***a** *ste4 FUS1-lacZ FUS1-HIS3 ura3-52 ssk1::NAT*	(51)

PC1531	*MAT***a** *ste4 FUS1-lacZ FUS1-HIS3 ura3-52 sho1::HYG*	(48)
PC1558	*MAT***a** *ste4 FUS1-lacZ FUS1-HIS3 ura3-52 sho1::HYG ssk1::NAT*	(7)
PC1625	*MAT***a** *ste4 FUS1-lacZ FUS1-HIS3 ura3-52 GAL-MSB2-HA::KanMX6::NAT GAL-SHO1::KanMX6*	(22)
PC1806	*MAT***a** *ste4 FUS1-lacZ FUS1-HIS3 ura3-52 GAL-MSB2-HAΔ100–818::KanMX6*	This study
PC1811	*MAT***a** *ste4 FUS1-lacZ FUS1-HIS3 ura3-52 MSB2-HAΔ100–818 ste12::URA3*	This study
PC1823	*MAT***a** *ste4 FUS1-lacZ FUS1-HIS3 ura3-52 GAL-MSB2-HA::KanMX6::NAT GAL-SHO1::KanMX6 leu2::HYG*	This study
PC1828	*MAT***a** *ste4 FUS1-lacZ FUS1-HIS3 ura3-52 GAL-MSB2-HA::KanMX6::NAT GAL-SHO1::KanMX6 rsr1::URA3*	This study
PC1895	*MAT***a** *ste4 FUS1-lacZ FUS1-HIS3 ura3-52 leu2:: HYG*	This study
PC2053	*MAT***a** *ste4 FUS1-lacZ FUS1-HIS3 ura3-52 pbs2::KanMX6*	(51)
PC2061	*MAT***a** *ste4 FUS1-lacZ FUS1-HIS3 ura3-52 ssk1::NAT ste11::URA*	(51)
PC2519	*MAT***a** *ste4 FUS1-lacZ::NAT FUS1-HIS3*	This study
PC2613	*MAT***a** *ste4 FUS1-lacZ FUS1-HIS3 ura3-52 trp1::NAT*	(52)
PC2710	*MAT***a** *ste4 FUS1-lacZ FUS1-HIS3 ura3-52 cdc12-6::NAT*	This study
PC3363	*MAT***a** *ste4 FUS1-lacZ FUS1-HIS3 ura3-52 bud2::KlURA3*	This study
PC3391	*MAT***a** *ste4 FUS1-lacZ FUS1-HIS3 ura3-52 rga1::NAT*	(7)
PC3619	*MAT***a** *ste4 FUS1-lacZ FUS1-HIS3 ura3-52 rax1::KlURA3*	This study
PC3629	*MATα ura3 leu2 axl1::LEU2*	This study
PC3631	*MAT***a** *ste4 FUS1-lacZ FUS1-HIS3 ura3-52 trp1::NAT axl1::TRP1*	This study
PC3633	*MAT***a** *ste4 FUS1-lacZ FUS1-HIS3 ura3-52 bud2::KlURA3*	This study
PC3635	*MAT***a** *ste4 FUS1-lacZ FUS1-HIS3 ura3-52 bud3::KlURA3*	This study
PC3797	*MAT***a** *ura3-52 rsr1::NAT*	This study
PC3798	*MATα ura3-52 rsr1::HYG*	This study
PC3800	*MATα ura3-52 rsr1::HYG/ MAT***a** *ura3-52 rsr1::NAT*	This study
PC3861	*MAT***a** *ste4 FUS1-lacZ FUS1-HIS3 ura3-52 ste11::NAT*	This study
PC3940	*MAT***a** *ste4 FUS1-lacZ FUS1-HIS3 ura3-52 rsr1::KlURA3 pbs2::NAT*	This study
PC3942	*MAT***a** *ste4 FUS1-lacZ FUS1-HIS3 ura3-52 rsr1::KlURA3 ssk1::NAT*	This study
PC4103	*MAT***a** *ste4 FUS1-lacZ FUS1-HIS3 ura3-52 axl2::NAT*	This study
PC4105	*MAT***a** *ste4 FUS1-lacZ FUS1-HIS3 ura3-52 trp1::NAT axl1::TRP1 rax1::KlURA3*	This study
PC4161	*MAT***a** *ste4 FUS1-lacZ FUS1-HIS3 ura3-52 trp1::NAT axl2::TRP1*	This study
PC4164	*MAT***a** *ste4 FUS1-lacZ FUS1-HIS3 ura3-52 trp1::NAT axl2::TRP1 rax1::KlURA3*	This study
PC4176	*MAT***a** *ste4 FUS1-lacZ FUS1-HIS3 ura3-52 axl2::NAT rax1::KlURA3*	This study
PC4248	*MAT***a** *ste4 FUS1-lacZ FUS1-HIS3 ura3-52 rax2::KanMX6*	This study
PC4250	*MAT***a** *ste4 FUS1-lacZ FUS1-HIS3 ura3-52 rax1::KlURA3 rax2::KanMX6*	This study
PC4252	*MAT***a** *ste4 FUS1-lacZ FUS1-HIS3 ura3-52 axl2::NAT rax2::KlURA3*	This study
PC4254	*MAT***a** *ste4 FUS1-lacZ FUS1-HIS3 ura3-52 axl2::NAT rax1::KlURA3 rax2::KanMX6*	This study
PC4256	*MAT***a** *ste4 FUS1-lacZ FUS1-HIS3 ura3-52 rsr1::NAT*	This study
PC4326	*MAT***a** *ste4 FUS1-lacZ FUS1-HIS3 ura3-52 rsr1::KlURA3 rga1::NAT*	This study
PC4328	*MAT***a** *ste4 FUS1-lacZ FUS1-HIS3 ura3-52 axl2::KlURA3 rga1::NAT*	This study
PC4330	*MAT***a** *ste4 FUS1-lacZ FUS1-HIS3 ura3-52 bud3::KlURA3 rax1::NAT*	This study

PC4332	*MAT***a** *ste4 FUS1-lacZ FUS1-HIS3 ura3-52 bud4::KlURA3 rax1::NAT*	This study
PC4371	*MAT***a** *ste4 FUS1-lacZ FUS1-HIS3 ura3-52 MSB2$^{\Delta 100\text{-}818}$ axl2::URA3*	This study
PC4674	*MAT***a** *ste4 FUS1-lacZ FUS1-HIS3 ura3-52 leu2::HYG rsr1::KlURA3*	This study
PC4970	*MAT***a** *ste4 FUS1-lacZ FUS1-HIS3 ura3-52 cdc24::NAT pRS316-CDC24*	(7)
PC5124	*MAT***a** *ste4 FUS1-lacZ FUS1-HIS3 ura3-52 leu2::HYG cdc24::NAT pYEP351-Cdc24p-GFP*	(7)
PC5125	*MAT***a** *ste4 FUS1-lacZ FUS1-HIS3 ura3-52 leu2::HYG cdc24::NAT pYEp351-MYR-Cdc24p-GFP*	(7)
PC5130	*MAT***a** *ste4 FUS1-lacZ FUS1-HIS3 ura3-52 leu2::HYG cdc24::NAT pYEp351-MYR-Cdc24p-GFP rsr1::NAT*	This study
PC6492 [b]	*MATα ste4 FUS1-HIS3 ura3-52 pmi40-101 rsr1:: URA3*	This study
PC6521	*MAT***a** *ste4 FUS1-lacZ FUS1-HIS3 ura3-52 msb2::KanMX6 rsr1:: KlURA3*	This study
PC6495 [b]	*MATα ste4 FUS1-HIS3 ura3-52 pmi40-101 axl1:: URA3*	This study
PC6533	*MAT***a** *ste4 FUS1-HIS3 FUS1-LacZ ura3-52 leu2::URA3 Bud3p-mCherry::KanMX6*	This study
PC6528	*MAT***a** *ste4 FUS1-lacZ FUS1-HIS3 ura3-52 BUD3-mCherry::KanMX6*	This study
PC6584	*MAT***a** *ste4 FUS1-lacZ FUS1-HIS3 ura3-52 leu2::HYG cdc24::NAT pYEp351-MYR-Cdc24p-GFP bud4::NAT*	This study

a. All strains are in the ∑1278b background unless otherwise indicated.
b. Strains derived from the 246-1-1 background (53).
c. Strains designated *ura3-* were generated by identifying colonies resistant to 5-FOA.
d. Cg refers to a gene from the species *Candida glabrata,* and Kl, *Kluyveromyces lactis*.

Table S2. Plasmids used in the study.

Name	Description	Reference
p151	p*AXL1-HA*	(20)
PC1405	p*FRE-lacZ*	(54)
PC1441	YCp50-*STE11-4*	(55)
PC1601	pRS316-*SHO1-GFP*	(56)
PC1614	pRS316-*SHO1-GFP* ^{D16H}	(56)
PC1696	p*GFP-MSB2*	(46)
PC1715	pRS316-*SHO1*$^{D16H\ P120L}$*-GFP*	(22)
PC1879	pGAL-*SHO1-GFP::KanMX6*	(22)
PC1882	pGAL-*SHO1*^{D16H}*-GFP::KanMX6*	(22)
PC1883	YEp*GFP-BUD8*	(57)
PC1422	pRS315	(Sikorski and Hieter 1989)
PC2150	pRS316-*CDC24*	This study
PC2151	pRS315-*CDC24*	This study
PC2205	p*NAT*	(13)
PC2206	p*HYG*	(13)
PC2207	pRS316	(15)
PC2220	pGAL-*SHO1-GFP*^{D16H}::KanMX6::NAT	This study
PC2241	pSM217-*GIC2-GFP*	(58)
PC2415	pFA6a-*mCherry-kanMX6*	(14)
PC2432	pRS316-*SHO1*^{D16H}*-HA::KANMX6*	This study
PC2433	pRS316-*SHO1*$^{D16H\ P120L}$*-HA::KANMX6*	This study
PC2435	pRS316-*SHO1* $^{D16H\ S220F}$*-HA::KANMX6*	This study
PC3621	pRS316-*CDC24-GFP*	Rong Li
PC4146	pRS426-*AXL2 1-823* (#235)	(16)
PC4147	pRS426-*AXL2 p1-646* (#238)	(16)
PC4149	pRS426-*AXL2 p1-544, 641-725* (#319)	(16)
PC4150	pRS426-*AXL2 p1-544, 641-685* (#320)	(16)
PC4151	pRS426-*AXL2 p1-544, 726-823* (#318)	(16)
PC4657	pRS425 2μ *LEU2*	(15)
PC5157	YEp351-*Cdc24p-GFP*	(7)
PC5161	YEp351-*MYR-Cdc24p-GFP*	(7)
PC6077	pRS315-*CDC24-4*	(7)
PC6078	pRS425-*CDC24-4*	(7)
pHP1118	YEplac195-*RSR1 (URA3*)	(17)
pHP1124	YEp1ac195- *rsr1*^{T35A}	(17)
pHP562	YEp13-*RSR1* (*LEU2*)	(18)
pHP596	YEp13- *rsr1*^{K16N}	(18)
pHP595	YEp13- *rsr1*^{G12V}	(18)
pHP1123	YEplac195-*rsr1-7*$^{K260\text{-}264S}$	(17)
pHP1755	YEplac195-*rsr1*-8K$^{260\text{-}261S}$	(19)
pHP1753	YEplac195-*rsr1*-9K$^{263\text{-}264S}$	(19)
pSW72	pRS315 (LEU/CEN) CDC24-GFP	(59)

Table S3. Budding pattern of *RSR1* alleles and the *rsr1*Δ mutant in combination with *rga1*Δ and *axl2*Δ.

Strain [a]	Proximal	Equatorial	Distal
Wild type	98	1	1
*rsr1*Δ	9	72.5	18.5
*rga1*Δ	36	11	53
*rga1*Δ *rsr1*Δ	17.5	57.5	25
*axl2*Δ	16	8	76
*rga1*Δ *axl2*Δ	15	4	81
*rsr1*Δ YEp13-*RSR1*	44	50	6
*rsr1*Δ YEp13-*rsr1* ^{G12V}	6	81	13
*rsr1*Δ YEp13-*rsr1* ^{K16N}	6	75	19
*rsr1*Δ YEplac195-*rsr1* ^{T35A}	8	77	15

a. Cells were grown to mid-log phase in YEPD medium to minimize polarized growth which can impact budding pattern (60, 61), and stained with CFW as described in the M&M. Budding pattern was determined by bud position and the position of bud scars, which occur at a low frequency in the *rga1*Δ mutant (62). >200 cells were counted for each experiment. Values are expressed as a percentage.

Table S4. Budding pattern of axial mutants alone and in combination with *rax1*Δ.[a]

Strain [b]	Proximal	Equatorial	Distal
Wild type	98	<1	2
*bud3*Δ	3	6	93
*bud3*Δ *rax1*Δ	57	17	26
*bud4*Δ	15	4	81
*bud4*Δ *rax1*Δ	61	4	35
*axl1*Δ	19	5	76
*axl1*Δ *rax1*Δ	92	1	7
*axl2*Δ [c]	10	6	84
*axl2*Δ *rax1*Δ	15	26	59

a. Cells were grown to mid-log phase in SD+AA medium (2% glucose).

b. >100 cells were counted for each mutant. Values are expressed as the percentage of cells exhibiting the indicated pattern.

c. Axl2p is the key axial landmark in haploids, and its loss cannot be bypassed by loss of Rax proteins (43, 44). The *rax1*Δ mutant failed to suppress the budding or MAPK signaling defects of the *axl2*Δ mutant (see also *Fig. S3D-E*).

A

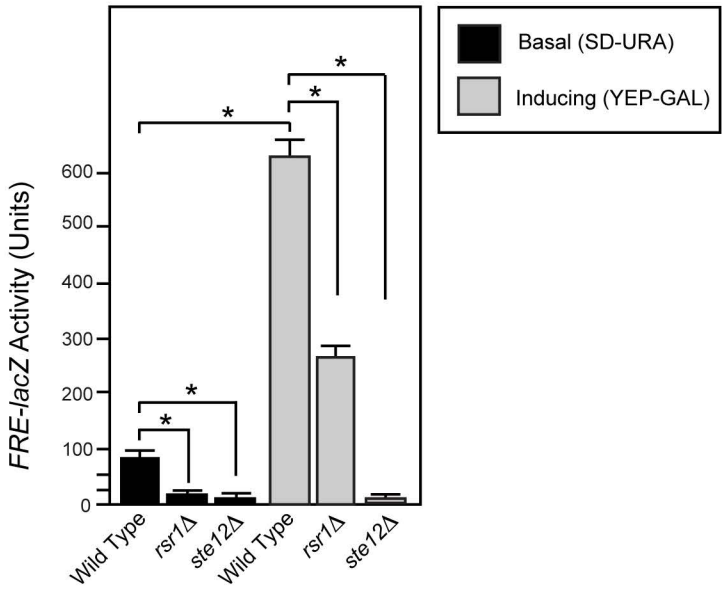
Basal (SD-URA)
Inducing (YEP-GAL)
FRE-lacZ Activity (Units)
0
100
200
300
400
500
600
*
*
*
*
*
Wild Type
rsr1Δ
ste12Δ
Wild Type
rsr1Δ
ste12Δ

B

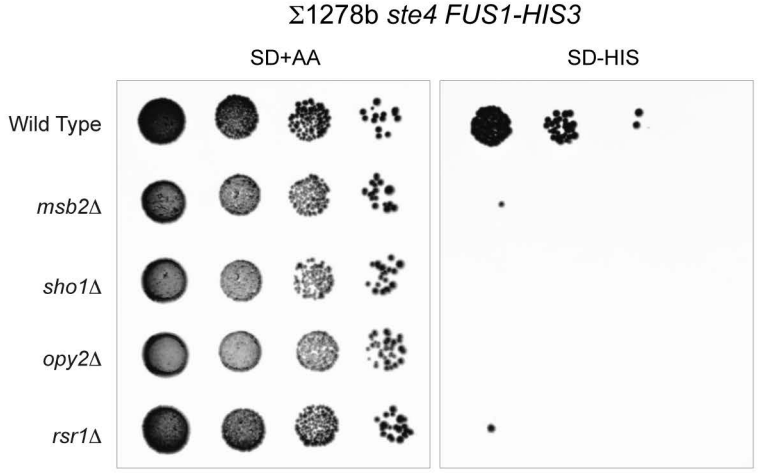
Σ1278b ste4 FUS1-HIS3
SD+AA
SD-HIS
Wild Type
msb2Δ
sho1Δ
opy2Δ
rsr1Δ

C

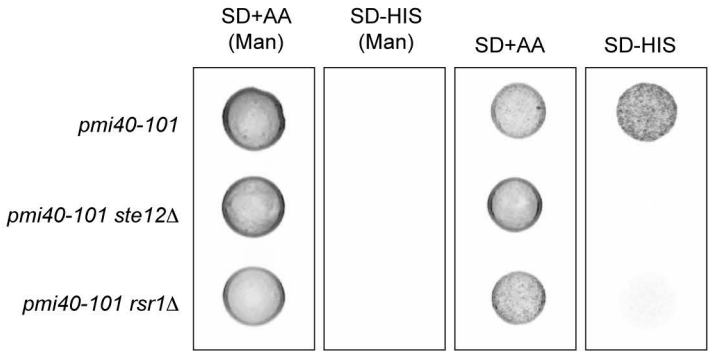
SD+AA (Man)
SD-HIS (Man)
SD+AA
SD-HIS
pmi40-101
pmi40-101 ste12Δ
pmi40-101 rsr1Δ

D

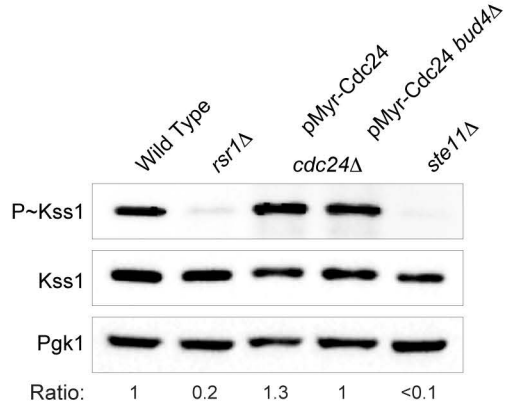
Wild Type
rsr1Δ
pMyr-Cdc24
cdc24Δ
pMyr-Cdc24 bud4Δ
ste11Δ
P~Kss1
Kss1
Pgk1
Ratio:
1
0.2
1.3
1
<0.1

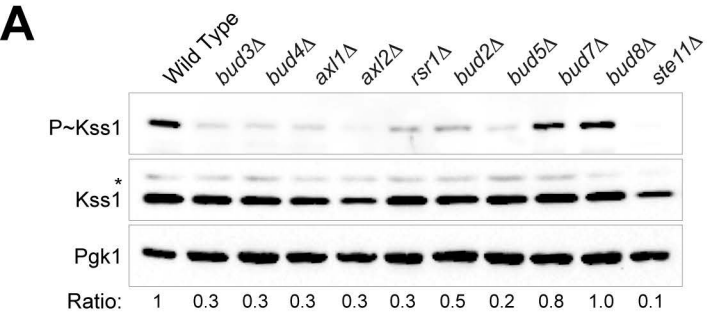
A
Wild Type
bud3Δ
bud4Δ
axl1Δ
axl2Δ
rsr1Δ
bud2Δ
bud5Δ
bud7Δ
bud8Δ
ste11Δ
P~Kss1
Kss1*
Pgk1
Ratio: 1 0.3 0.3 0.3 0.3 0.3 0.5 0.2 0.8 1.0 0.1

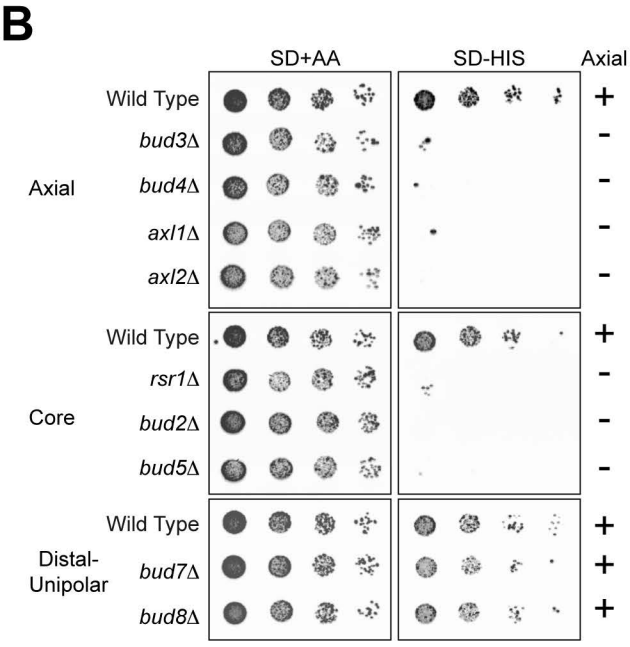
B
SD+AA
SD-HIS
Axial
Wild Type
bud3Δ
bud4Δ
axl1Δ
axl2Δ
Axial
Wild Type
rsr1Δ
bud2Δ
bud5Δ
Core
Wild Type
bud7Δ
bud8Δ
Distal-Unipolar

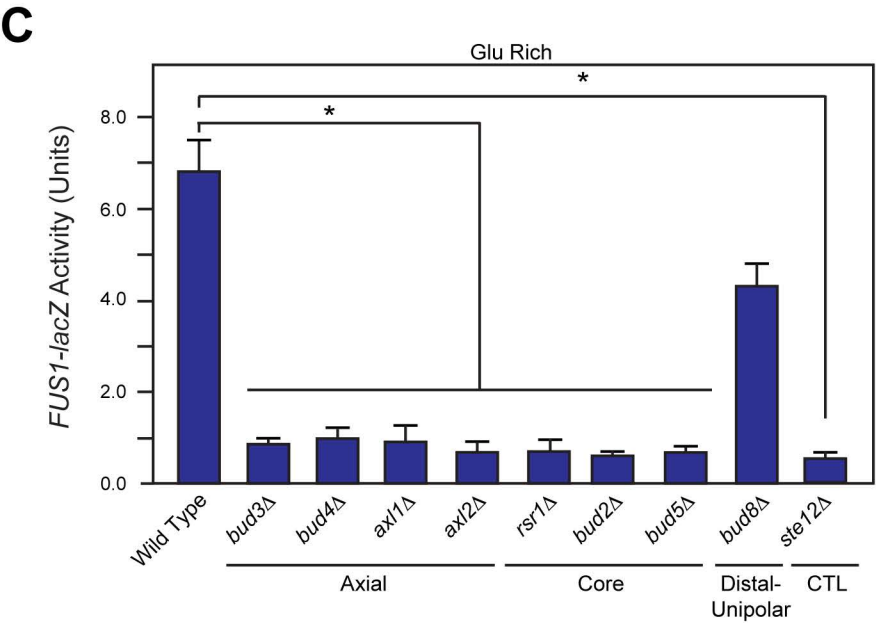
C
Glu Rich
FUS1-lacZ Activity (Units)
8.0
6.0
4.0
2.0
0.0
Wild Type
bud3Δ
bud4Δ
axl1Δ
axl2Δ
rsr1Δ
bud2Δ
bud5Δ
bud8Δ
ste12Δ
Axial
Core
Distal-Unipolar
CTL

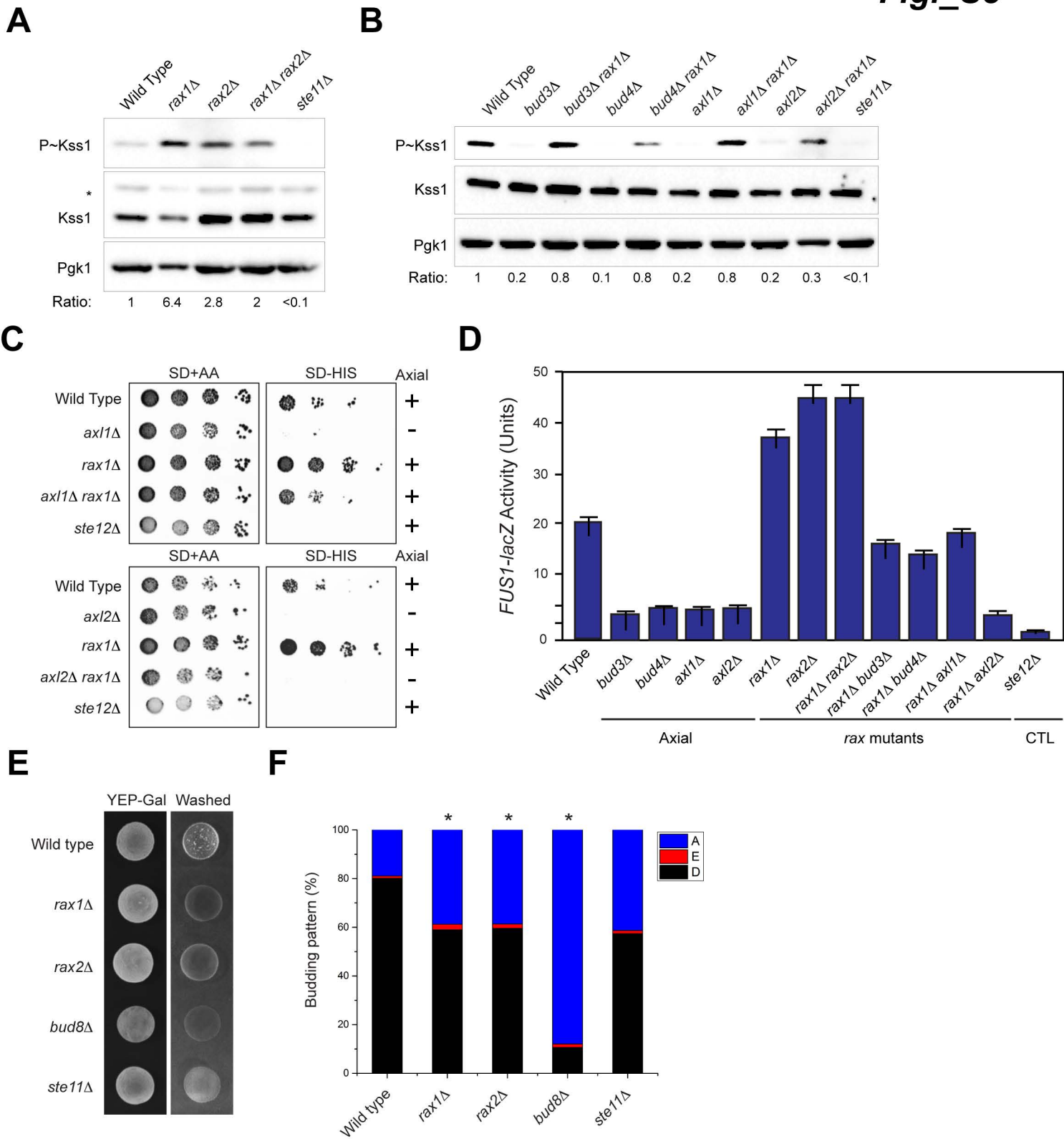
A
Wild Type
rax1Δ
rax2Δ
rax1Δ rax2Δ
ste11Δ
P~Kss1
*
Kss1
Pgk1
Ratio: 1 6.4 2.8 2 <0.1
B
Wild Type
bud3Δ
bud3Δ rax1Δ
bud4Δ
bud4Δ rax1Δ
axl1Δ
axl1Δ rax1Δ
axl2Δ
axl2Δ rax1Δ
ste11Δ
P~Kss1
Kss1
Pgk1
Ratio: 1 0.2 0.8 0.1 0.8 0.2 0.8 0.2 0.3 <0.1
C
SD+AA
SD-HIS
Axial
Wild Type
axl1Δ
rax1Δ
axl1Δ rax1Δ
ste12Δ
SD+AA
SD-HIS
Axial
Wild Type
axl2Δ
rax1Δ
axl2Δ rax1Δ
ste12Δ
D
FUS1-lacZ Activity (Units)
0
10
20
30
40
50
Wild Type
bud3Δ
bud4Δ
axl1Δ
axl2Δ
rax1Δ
rax2Δ
rax1Δ rax2Δ
rax1Δ bud3Δ
rax1Δ bud4Δ
rax1Δ axl1Δ
rax1Δ axl2Δ
ste12Δ
Axial
rax mutants
CTL
E
YEP-Gal
Washed
Wild type
rax1Δ
rax2Δ
bud8Δ
ste11Δ
F
Budding pattern (%)
0
20
40
60
80
100
*
*
*
A
E
D
Wild type
rax1Δ
rax2Δ
bud8Δ
ste11Δ

Fig._S4

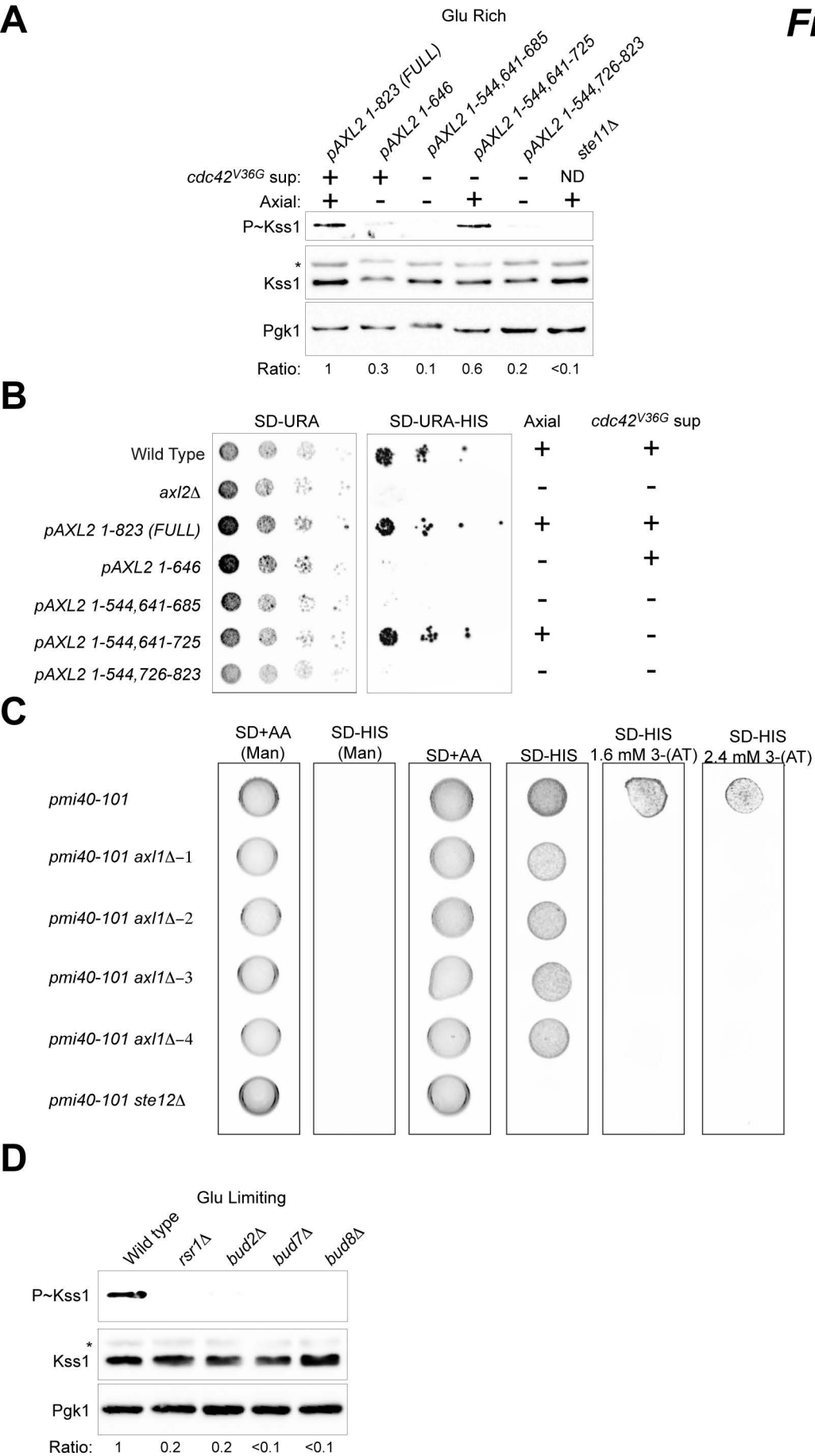
A
Glu Rich
pAXL2 1-823 (FULL)
pAXL2 1-646
pAXL2 1-544,641-685
pAXL2 1-544,641-725
pAXL2 1-544,726-823
ste11Δ
cdc42V36G sup: + + - - - ND
Axial: + - - + - +
P~Kss1
*
Kss1
Pgk1
Ratio: 1 0.3 0.1 0.6 0.2 <0.1
B
SD-URA
SD-URA-HIS
Axial
cdc42V36G sup
Wild Type + +
axl2Δ - -
pAXL2 1-823 (FULL) + +
pAXL2 1-646 - +
pAXL2 1-544,641-685 - -
pAXL2 1-544,641-725 + -
pAXL2 1-544,726-823 - -
C
SD+AA (Man)
SD-HIS (Man)
SD+AA
SD-HIS
SD-HIS 1.6 mM 3-(AT)
SD-HIS 2.4 mM 3-(AT)
pmi40-101
pmi40-101 axl1Δ–1
pmi40-101 axl1Δ–2
pmi40-101 axl1Δ–3
pmi40-101 axl1Δ–4
pmi40-101 ste12Δ
D
Glu Limiting
Wild type
rsr1Δ
bud2Δ
bud7Δ
bud8Δ
P~Kss1
*
Kss1
Pgk1
Ratio: 1 0.2 0.2 <0.1 <0.1

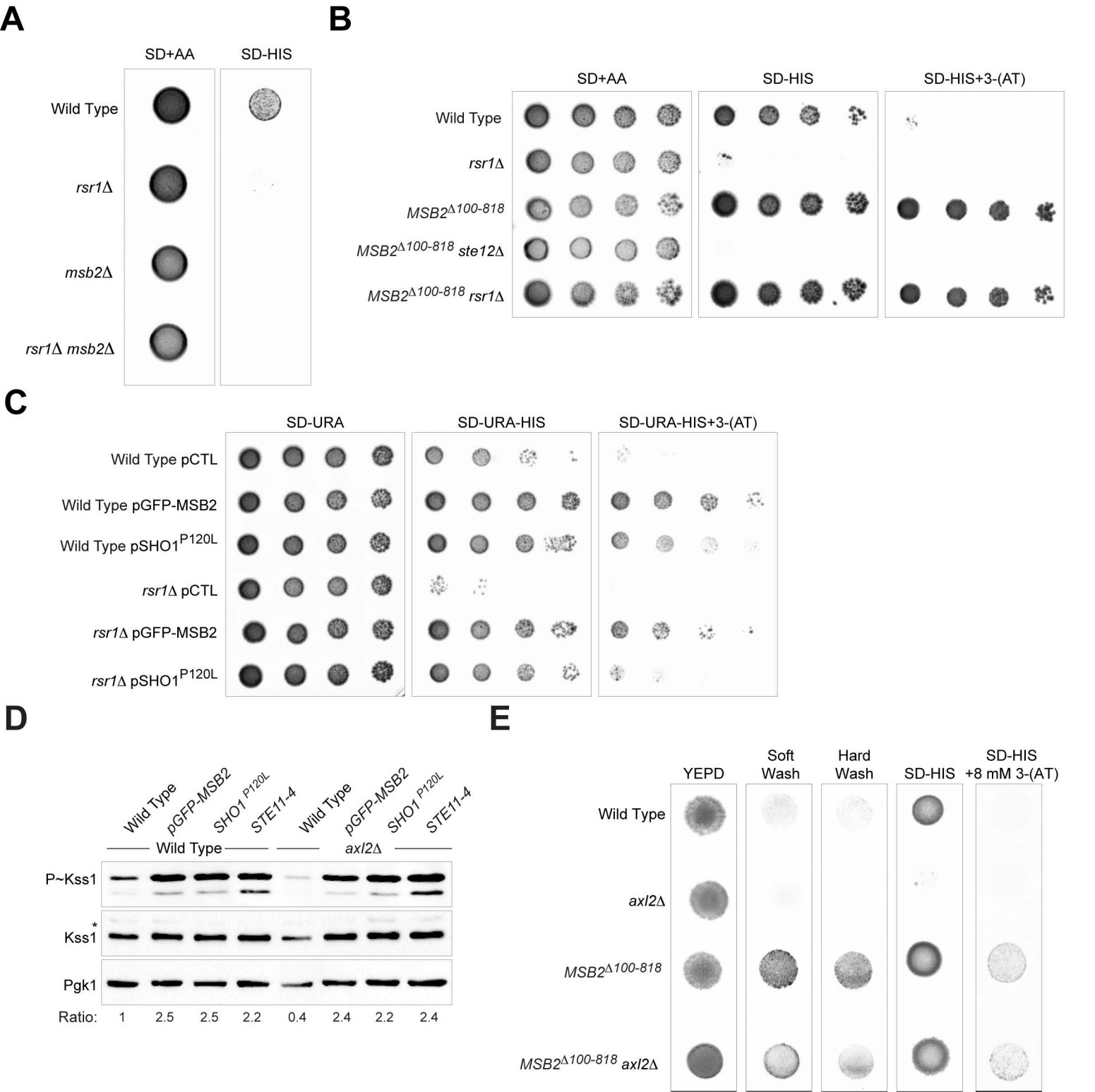
A
SD+AA
SD-HIS
Wild Type
rsr1Δ
msb2Δ
rsr1Δ msb2Δ
B
SD+AA
SD-HIS
SD-HIS+3-(AT)
Wild Type
rsr1Δ
MSB2Δ100-818
MSB2Δ100-818 ste12Δ
MSB2Δ100-818 rsr1Δ
C
SD-URA
SD-URA-HIS
SD-URA-HIS+3-(AT)
Wild Type pCTL
Wild Type pGFP-MSB2
Wild Type pSHO1P120L
rsr1Δ pCTL
rsr1Δ pGFP-MSB2
rsr1Δ pSHO1P120L
D
Wild Type
pGFP-MSB2
SHO1 P120L
STE11-4
Wild Type
pGFP-MSB2
SHO1 P120L
STE11-4
Wild Type
axl2Δ
P~Kss1
Kss1*
Pgk1
Ratio:
1
2.5
2.5
2.2
0.4
2.4
2.2
2.4
E
YEPD
Soft Wash
Hard Wash
SD-HIS
SD-HIS +8 mM 3-(AT)
Wild Type
axl2Δ
MSB2Δ100-818
MSB2Δ100-818 axl2Δ

Fig._S6

A

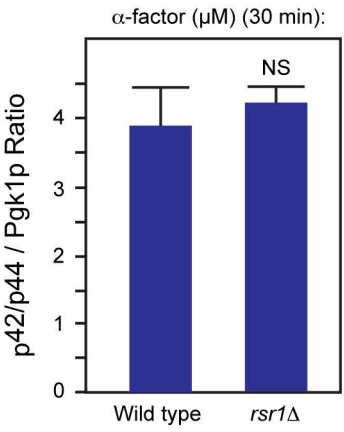
α-factor (μM) (30 min):
NS
p42/p44 / Pgk1p Ratio
0
1
2
3
4
Wild type
rsr1Δ

B

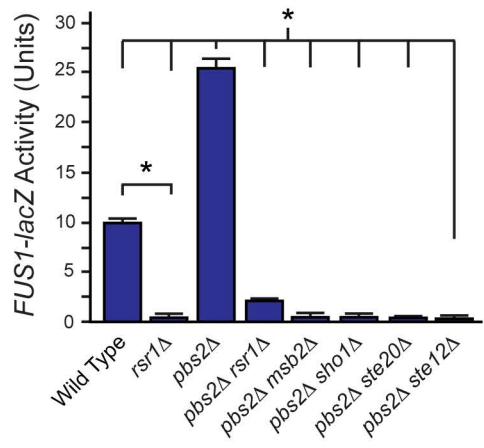
FUS1-lacZ Activity (Units)
0
5
10
15
20
25
30
*
*
Wild Type
rsr1Δ
pbs2Δ
pbs2Δ rsr1Δ
pbs2Δ msb2Δ
pbs2Δ sho1Δ
pbs2Δ ste20Δ
pbs2Δ ste12Δ

C

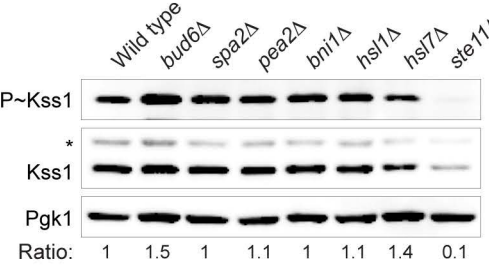
Wild type
bud6Δ
spa2Δ
pea2Δ
bni1Δ
hsl1Δ
hsl7Δ
ste11Δ
P~Kss1
*
Kss1
Pgk1
Ratio: 1 1.5 1 1.1 1 1.1 1.4 0.1

Fig._S7

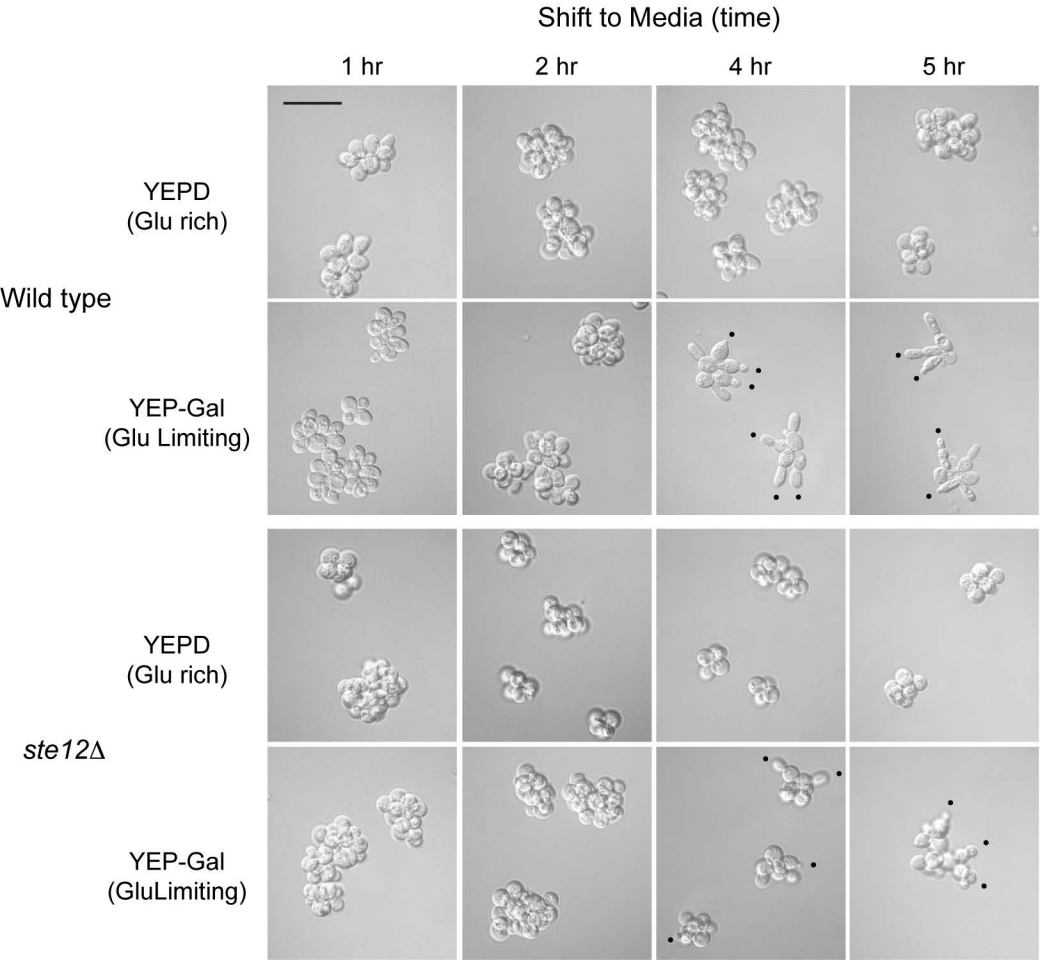
Shift to Media (time)
1 hr
2 hr
4 hr
5 hr
YEPD
(Glu rich)
Wild type
YEP-Gal
(Glu Limiting)
YEPD
(Glu rich)
ste12Δ
YEP-Gal
(GluLimiting)

Fig._S8

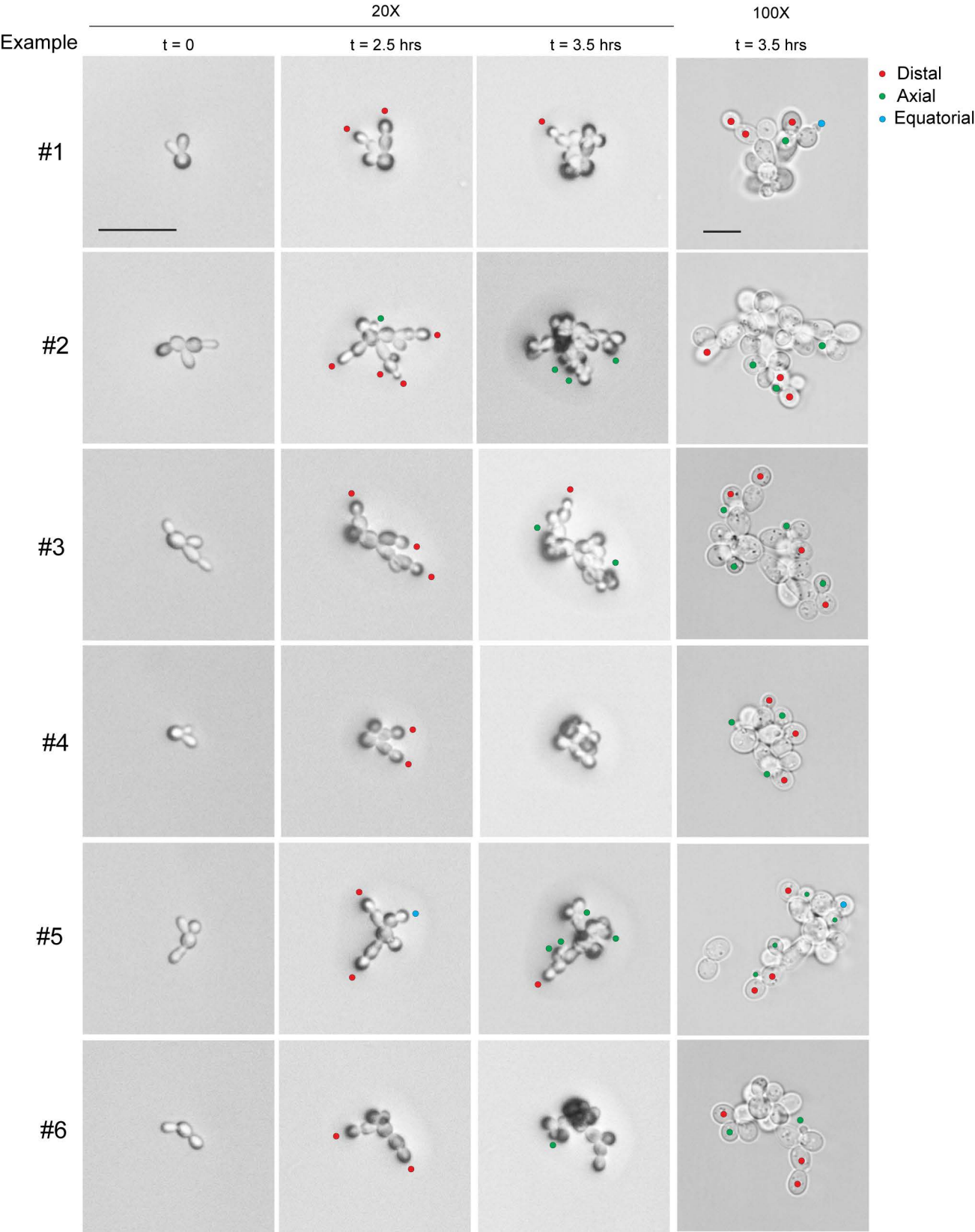
20X
100X
Example
t = 0
t = 2.5 hrs
t = 3.5 hrs
t = 3.5 hrs
Distal
Axial
Equatorial
#1
#2
#3
#4
#5
#6

Fig._S9